Journal of Quantitative Spectroscopy & Radiative Transfer 242 (2020) 106747

Contents lists available at ScienceDirect

Journal of Quantitative Spectroscopy & Radiative Transfer

journal homepage: www.elsevier.com/locate/jqsrt

Consistent Franck–Condon modeling of geometry changes for the $S_0 \rightarrow S_1(\pi\pi^*)$ excitation in anthranilic acid: LIF spectroscopy aided by CC2 or TDDFT vibrations

Przemysław Kolek[a,*], Marcin Andrzejak[b], Tomasz Uchacz[c], Paweł Szlachcic[d]

[a] Department of Experimental Physics, Faculty of Mathematics and Natural Sciences, University of Rzeszów, 1 Pigonia Street, PL-35-310 Rzeszów, Poland
[b] K. Gumiński Department of Theoretical Chemistry, Faculty of Chemistry, Jagiellonian University, Gronostajowa 2, PL-30-387 Kraków, Poland
[c] Department of Physical Chemistry, Faculty of Chemistry, Jagiellonian University, Gronostajowa 2, PL-30-387 Kraków, Poland
[d] Institute of Chemistry, Faculty of Food Technology, Agricultural University, ul. Balicka 122, PL-31-149 Kraków, Poland

ARTICLE INFO

Article history:
Received 3 July 2019
Revised 2 November 2019
Accepted 5 November 2019
Available online 6 November 2019

Keywords:
Excited-state geometry
Franck–Condon analysis
LIF laser-induced fluorescence excitation spectra
CC2 coupled-cluster
TDDFT
Vibrational analysis

ABSTRACT

Experimentally-based evaluation of the changes of equilibrium geometry for the $S_0 \rightarrow S_1(\pi\pi^*)$ excitation in anthranilic acid via fitting of Franck–Condon factors is tested for reliability. The modeling is based on the experimental band intensities in the LIF spectrum that are transformed into geometry changes with the aid of the vibrational modes computed using both the CC2 method (the perturbative approximation to CCSD coupled-cluster) and TDDFT(B3LYP). This modeling is a challenging task not only for quantitative spectroscopy, but also for the quantum chemistry calculations, since the adequate reproduction of vibrational modes for the excited state requires a balanced treatment of the π-electronic conjugation and dynamic electron correlation. The most reliable approach (LIF+CC2 Franck–Condon fitting) predicts a dramatic shortening of the O···H distance by 31 ± 1.5 pm, from 1.91 Å in the ground state to 1.60 Å in the excited state. The changes in bond alternation in the H-chelate ring (around 5 pm according to the LIF+CC2 fit) and the shortening of the O···H bond are typically 1 pm larger than modeled with the LIF+TDDFT fit. Changes of valence angles of magnitude around 5° are larger by 0.5°-1.0° according to LIF+CC2 FC fit than the LIF+DFT fit. Consistency of the obtained results shows that the Franck-Condon fitting provides a reliable, experimentally-based approach to evaluation of the excitation-related geometry changes. It has been achieved owing to the quantitatively reliable spectroscopic results and vibrational analysis computed using the quantum chemistry methods that are able to provide correct description of the excited-state vibrational modes involving the intramolecular hydrogen bond.

1. Introduction

Investigation of molecular geometry in the excited electronic states is one of the important issues of molecular spectroscopy and photochemistry, since it provides insight into the properties of the excited molecules and the changes imposed by excitation. Various approaches to ab initio modeling of vibronic structure for UV–vis absorption or fluorescence bands for aromatic molecules were extensively studied [1–7] within Franck–Condon and/or Hertzberg–Teller model. Tentative considerations of geometry changes bases on the activity of vibronic bands are very popular in photochemistry and spectroscopy. On the other hand, the quantitatively reliable evaluation of geometry changes on the basis of intensities for vibronic bands in experimental spectra [8–10] is not straightforward and is carried out rather rarely. This is due to several limitations of the UV/vis spectroscopy and *ab initio* vibrational analysis of polyatomic molecules in excited states. Unfortunately, limited resolution of absorption or emission spectra of solid or liquid samples is usually insufficient for the resolving of a reach vibrational structure of electronic transition generated by the activity of the low-frequency oscillations. High spectral resolution is achievable for molecules cooled in supersonic-jet expansion in the spectra recorded using techniques of laser spectroscopy (e.g. laser-induced fluorescence LIF, resonantly enhanced multiphoton ionization REMPI).

The fitting of FC factors in order to reproduce the vibrationally resolved UV spectra is based on fitting of the displacement parameters along the normal coordinates. Within this very modeling all these parameters can be treated as abstract numbers but for the evaluation of the geometry changes upon excitation these

* Corresponding author.
E-mail addresses: pkolek@univ.rzeszow.pl, pkolek@ur.edu.pl (P. Kolek).

https://doi.org/10.1016/j.jqsrt.2019.106747
0022-4073/

parameters ought to be transformed into changes of the Cartesian geometry or into changes of the internal coordinates. Thus, the FC modeling of geometry changes in polyatomic molecules relies not only on the experimental data but also on the molecular vibrations computed using high-level quantum chemistry methods [8–10]. For the Franck–Condon modeling of high-resolution absorption or excitation spectra and geometry changes, the quantitatively accurate calculations of the excited-state vibrational modes are essential even though it can be a challenging task from the quantum chemistry point of view.

Anthranilic acid AA (*ortho*-aminobenzoic acid) is an aromatic molecule in which the $\pi \rightarrow \pi^*$ excitation causes significant strengthening of the intramolecular hydrogen bond. Its peculiar photochemical properties [11–13] make AA an interesting model system for spectroscopic investigations of the properties of hydrogen bond in excited states [14,15] as well as a useful tool in biological research, especially as a fluorescent probe in internally quenched fluorescent peptides for investigations involving fluorescence resonance energy transfer (FRET) processes [11,12]. The strengthening of the intramolecular hydrogen bond in π-conjugated molecules often causes appearance of dual fluorescence, which is traditionally interpreted as the evidence for the excited-state intramolecular proton transfer ESPIT (originally proposed by Weller in 1960s for salicylic acid and methyl salicylate [16]). Later, UV [17–20] spectroscopy and resonance Raman studies [21] and femtosecond spectroscopy [22] showed that skeleton relaxation involving low-frequency vibrational modes [19] plays an important role in the ESIPT process, while the magnitude of hydrogen atom dislocation is only 0.1–0.2 Å [19] in salicylic acid and its derivatives. Quantum chemistry calculations indicated that the actual process in these molecules is the skeletal relaxation accompanied not by the total hydrogen atom transfer, but rather by its significant dislocation [23–25]. On the other hand, polar solvents and proton acceptors or donors facilitate the appearance of strongly Stokes-shifted dual fluorescence in solutions [13,20] also in protonated forms of anthranilic acid [13]. This indicates that polar environment is able to stabilize the highly polar internally H-bonded tautomers in excited states (the ESIPT state). Because the N–H···O hydrogen bond is not so strong as the O–H···O bond, most of the interesting spectroscopic and physicochemical phenomena observed and extensively investigated for salicylic acid derivatives, are also present in AA, but in smaller magnitude.

AA is a convenient model molecule for the investigation of the interplay of the shortening of the hydrogen bond, skeletal relaxation, and the hydrogen atom dislocation along the hydrogen bond because of several features that are important from the point of view of spectroscopy and quantum chemistry. Firstly, the geometry relaxation takes place on the single potential energy surface PES [26] without any barrier in the vicinity or between the equilibrium geometries of the ground state and the excited state or transition to another excited state PES, thus assuring that the intensity distribution in the excitation spectrum depends solely on the FC factors. This feature is also consistent with the results of modeling of excited-state PES for many molecules emitting dual fluorescence (interpreted as the result of ESPIT process), including salicylic acid [24,25] and related systems. Secondly, according to spectroscopic results [14] the intersection of the $S_1(\pi\pi^*)$ state with the S_2(n-π^*) state is certainly not present up to at least 2000 cm^{-1} above the origin band of the investigated $S_0 \rightarrow S_1$ transition. Moreover, our ab initio calculations (see Section 3) indicate that the separation between the $S_1(\pi$-$\pi^*)$ and the S_2(n-π^*) excited states is larger than 1 eV. Such intersections of states are often present in the π-conjugated internally H-bonded molecules [18,27] and they may be accessible with rather low excess of vibrational energy (400–1500 cm^{-1}) above the minimum of the π-π^* excited state. In those cases the internal conversion from the π-π^* excited state to the n-π^* state makes the LIF excitation spectrum terminate abruptly at certain excitation energy, because these molecules subsequently undergo radiationless internal conversion from the n-π^* state to the ground state [17,27]. Thirdly, extensive supersonic-jet studies provided data concerning the activity of the excited state vibrational modes in the excitation spectra (LIF [14,28] and REMPI [14,29]), as well as the changes of frequencies of the N–H stretches upon the excitation (Fluorescence-Dip IR-UV spectra [14]). The study of band intensities in the LIF spectrum of AA [28] and FC modeling [30] proved that they are determined predominantly by the displacement parameters for the normal modes that are related to the changes of equilibrium geometry upon the electronic excitation, while the influence of frequency changes and Dushinsky effect is small. The assignment of vibronic bands in the spectrum is supported by the analysis of LIF spectra of AA molecules deuterated in various positions in functional groups. [31–33] The FC analysis showed that the band intensities computed on the basis of the HF and CIS results, and hence the geometry changes, are severely underestimated [28,30]. The DFT(B3LYP) and TDDFT calculations for the AA molecule predict significantly larger FC factors, though still considerably too small. [30]

Although all *ab intio* results, as well as the Franck–Condon fits, predict that the largest geometry change upon the excitation in AA molecule is the shortening of the N–H···O hydrogen bond, substantial discrepancies concern the magnitude of this change. Hartree-Fock+CI Singles (CIS), for the S_0 and S_1 state respectively, predicted the shortening of the hydrogen bond by only 14.6 pm [30] while the DFT+TDDFT(B3LYP)/cc-pVDZ methods predicts shortening by 22.8 pm [26]. Recently, the CC2 calculations with the aug-cc-pVTZ and cc-pVQZ basis sets yielded the largest ab initio prediction of the hydrogen bond shortening equal to 27.3–27.4 pm [34], which is close to the FC fit aided by TDDFT vibrational analysis [30] (30.2–32.0 pm). The FC-fits based on the LIF spectrum predicted significantly larger geometry changes 17.2–19.5 pm (FC-fit aided by HF+CIS vibrational modes) and 30.2–32.0 pm (FC-fit aided by DFT+TDDFT vibrations [30]) but the discrepancy between the obtained results increased as well. Obviously, the fitting of FC factors to the experimental band intensities could be regarded as reliable experimentally-based approach to evaluation of the changes of equilibrium geometry upon electronic excitation provided that the values obtained when FC approach aided by vibrational analysis using various relevant ab initio methods are consistent.

In this paper we present the consistent experimentally-based evaluation of the changes of equilibrium geometry upon the $S_0 \rightarrow S_1(\pi\pi^*)$ excitation in π-conjugated AA based on the Franck–Condon fitting of the band intensities to the experimental LIF spectrum. The evaluation of geometry changes is aided by vibrational modes computed using two high-level methods: the CC2 coupled-cluster [34] and TDDFT(B3LYP) with a series of correlation consistent basis sets.

2. Experimental

There are a limited number of experimental techniques facilitating the determination of excited-state geometries for polyatomic molecules. Evaluation of geometry parameters on the basis of rotationally resolved spectra is feasible [10], however, it is not always conclusive even for small molecules, since the complete set of spectra for isotopic molecules it required. Spectra of molecules that consist about ten atoms could be rotationally resolved only for molecules of high symmetry and provided that spectral broadening [35-37] is small. The approach feasible for larger polyatomic molecules is the evaluation of the changes of equilibrium geometry upon the excitation based on Franck-Condon modeling of vibrationally resolved UV spectra [9].

We have based FC analysis of band intensities on the LIF excitation spectrum rather than the dispersed fluorescence spectrum because of the reasons mentioned below. The widths of rotational profiles in the excitation spectra of AA available in the literature were around 4–5 cm^{-1} (LIF [14] and REMPI [29]) and after optimization of cooling conditions in supersonic jet expansion the bandwidths were reduced to 1.4–2.0 cm^{-1}, similarly as shown articles. [28,31,32] In contrast to the above, the spectral resolution of the dispersed fluorescence spectra of AA [14] is much lower (22–33 cm^{-1}) due to the use of monochromator with rather wide aperture, which is necessary for the spectral analysis of the weak signal of fluorescence emitted by the AA molecules diluted in gas phase at very low pressure. Owing to the enhanced spectral resolution, more than 70 vibronic bands of AA are discernible and interpreted in the LIF spectrum [28] facilitating assignment of more than ten fundamental transitions of totally-symmetric vibrations and some overtones of out-off-plane modes, while in the relevant spectral range of the dispersed fluorescence spectra [14] only about 15 vibronic bands are discernible and only four fundamentals were identified. Thus, LIF excitation spectrum provides the data concerning plentiful vibronic bands, which facilitate crosschecking of the experimentally-determined displacement parameters for many vibrational modes. Moreover, many bands appear in groups for which separation between each other is smaller than 25 cm^{-1} (some bands above 350 cm^{-1} and almost all vibronic bands starting from 750 cm^{-1} above the origin band in the excitation spectra [14,28,29]). Since the resolution of the dispersed fluorescence spectra is lower by roughly order of magnitude than in excitation spectra, such bands (which obviously exist also in dispersed fluorescence of AA) could not be resolved. Nevertheless, the dispersed fluorescence spectra would facilitate straightforward interpretation of geometry changes in terms of the ground-state vibrations but only for three or four low-frequency oscillations.

In order to determine the experimental band intensities in the LIF excitation spectrum with possibly small error 10 scans of the LIF spectra were recorded with data averaging of 10 laser shots per point. For each laser shot the recorded fluorescence signal was normalized using the intensity of the excitation UV beam passing through the vacuum chamber that was measured with the photodiode collecting the UV light scattered on a matt plate. The error of band intensities in the averaged LIF spectrum recorded this way is roughly ±0.05 for band intensities normalized to the intensity of the origin band, $I_{00} = 1$ (±5 for I_{00} normalized to 100).

For the supersonic free jet expansion the pulsed electromagnetic valve (Parker) was used with the nozzle of internal diameter of the orifice equal to 0.8 mm. Helium at total pressure 5 bars (4 bars in addition to the atmospheric pressure) dried using a liquid nitrogen trap was used as the carrier gas. The pulsed free jet (10 pulses per second) was injected into the vacuum chamber towards a baffler and a strong diffusion pump (pumping speed 2000 L/s) backed by rotary pump. The oven mounted close to the pulsed valve contained ca. 0.5 cm^3 of milled AA sample and was heated to 80 °C while the nozzle was kept at the temperature 90 °C. This allowed for obtaining sufficiently high concentration of AA vapor in the jet and simultaneously to avoid dimerization of salicylic acid in gas phase [14,31] (typical for carboxylic acid molecules). Only a few band of the AA dimer approach 5% of the intensity of the monomer origin band and intensity of several weaker bands do not exceed 3% of this intensity. To assure high purity of the sample of AA was purified by three sequent recrystallizations from ethanol and subsequently, by sublimation under vacuum at 140 °C. The pure AA have been obtained as colorless crystals melting at 148–149 °C.

The laser beam used for the excitation of the laser induced-fluorescence crossed the supersonic jet ca 30 mm downstream form the nozzle orifice. The 2nd harmonic ($\lambda = 532$ nm, $\tau = 5$ ns, repetition rate 10 Hz) of the Quantell Brilliant B Nd:YAG laser was used for pumping of the tunable dye laser (Quantell TDL+, with grating having 2400 lines/mm) of spectral resolution better than 0.08 cm^{-1} in the visible range. The tunable UV extension of the Quantell TDL+ laser was used to obtain the tunable UV beam of resolution ca. 0.15 cm^{-1} via second harmonic generation. The dye laser ran on the LDS698(Exciton) dye up to 950 cm^{-1} over the origin band (29,591 cm^{-1}) and on DCM dye in the range 850–1600 cm^{-1} above the origin band. The recorded spectral ranges were assembled together using the least square method.

In order to avoid saturation and power broadening often appearing in the spectra of extremely diluted gas phase test scans of selected bands were recorded which shows that saturation and broadening become significant at powers exceeding 150 μJ per pulse (the diameter of laser beam was ca. 5 mm). To reduce the energy of the UV laser beam avoiding the increase the power fluctuations quartz plates were used instead of right angle prisms for conducting the laser beam into the vacuum chamber giving finally around 1% of the initial energy of the UV beam, thus the UV pulses of energy below 100 μJ per pulse were used for the final experiment. Bandwidths (FWHM) of rotational profiles of typically 1.4–2.0 cm^{-1} were achieved.

3. Computational details

High-quality vibrational modes for polyatomic molecules in the excited electronic state are needed for the inverse Franck-Condon analysis of the LIF excitation spectra that yield the changes of equilibrium geometry upon the excitation. For proper description of vibrational modes of hydrogen-bonded molecules major part of dynamic correlation effects should be included in the *ab initio* methods [23–25] used for the vibrational analysis. There are a limited number of methods applicable for excited electronic states of aromatic chromophores (such as AA) facilitating the full geometry optimization and subsequently the excited-state vibrational analysis at the level of theory that consistently includes electron correlation effects for both the ground state and the excited state.

According to the CC2 as well as TDDFT(B3LYP) results computed with (aug)-cc-pVXZ(X = D,T,Q) basis sets, the S_1 excited state of AA is dominated by the singly-excited electronic configurations (mainly the $\pi \rightarrow \pi^*$ HOMO-LUMO one) and it has a moderate oscillator strength ($f \approx 0.1$). The computed vertical excitation energies are within the range 3.8–4.0 eV, and noticeably, the ZPE-corrected transition energies [34] show very good agreement with the experimental data [13,14,28,29]. Similarly as in salicylic acid [25], the $S_1(\pi \rightarrow \pi^*)$ state is well separated from other excited singlet-states, by 1 eV vertically for the S_0 equilibrium geometry and by ca. 1.4 eV for the geometry optimized for this state, which indicate that Hertzberg-Teller vibronic coupling should not influence the vibrational structure of the $S_0 \rightarrow S_1$ absorption band. The vertical excitation to the $S_2(n \rightarrow \pi^*)$ state of A" symmetry has energy 4.8–5.0 eV. Additionally, there are four other states of A" symmetry having energies up to 6 eV, all of them with negligible oscillator strengths. In this energy range there are two other $\pi \rightarrow \pi^*$ transitions with energies 5.0–5.2 eV and 5.5–5.8 eV, the former with a small oscillator strength ($f \approx 0.035$) but the later one with a quite substantial intensity ($f \approx 0.35$). Also CASSCF calculations with 8 electrons correlated and 7 orbitals active indicate the same energetic order of the above states. These results indicate that the investigated S_1 state is the L_a state in Platt notation and the remaining $\pi \rightarrow \pi^*$ excited states are of L_b and B_b character, respectively. The ab initio results suggest that two absorption bands that are discernible in the UV absorption spectra in cyclohexane solution [13] at $\lambda_{1,max} = 333$ nm and $\lambda_{2,max} = 247$ nm (3.7 eV and 5.0 eV) should be assigned to the $S_0 \rightarrow L_a$ and $S_0 \rightarrow B_b$ transitions, respectively, while the weak $S_0 \rightarrow L_b$ transition band is probably obscured.

Nowadays, the most popular method applicable for vibrational analysis for the $\pi \rightarrow \pi^*$ HOMO-LUMO excitations in the AA molecule is the time-dependent perturbation scheme build on the density functional theory TDDFT. The advantage of the TDDFT treatment of single excitations is approximate inclusion of dynamical correlation at a rather low computational cost. The TDDFT(B3LYP) approach was found useful for the studies of vibronic structure of UV spectra for aromatic chromophores [1–10] and for studies of ESIHT process (hydrogen atom dislocation) in SA, AA and other π-conjugated and internally H-bonded molecules [24,26] and for the modeling of FC parameters in AA [30]. Our calculations using TDDFT method were carried out using the Gaussian 09 package [38].

Recently, CC2 [39–41] calculations became practically feasible for aromatic fluorophores. The CC2 method is the approximation of single-double coupled-cluster CCSD, in which single excitations fundamental for the description of excited states are fully included in the weavefunction, while contributions of double excitations essential for dynamical correlation are introduced perturbatively (in analogy to MP2). The CC2 calculations (scaling as N^5, N being the number of basis functions) are more computationally demanding than TDDFT (~N[3,4]), but they are less costly than the full CCSD scheme (~N[6]). The CC2 results are surprisingly accurate (often surpassing CCSD) for excitation energies, molecular geometries and harmonic frequencies [40,41] provided the wave function of the excited state is dominated by the singly-excited configurations. The nearly quantitative reproductions of the phosphorescence spectra of several organic chromophores of sizes similar to AA based on CC2 results confirm high quality of the CC2 method [2,9,10,42,43]. Our computations were done using currently available implementation of CC2 in Turbomole 6.3 package [44].

Vibrational frequency calculations for the ground and the excited state with the CC2 and the TDDFT for the excited state were carried out by numerical differentiation of analytical gradient. The ground-state vibrational analysis using DFT(B3LYP) method was carried out with analytical Hessian. All CC2 and TDDFT calculations were done with the series of the Dunning correlation consistent basis sets cc-pVXZ(X = D,T,Q) and aug-cc-pVXZ(X = D,T).

4. Calculations of Franck–Condon factors and fitting of geometry changes

State-of-the-art evaluation of Franck–Condon overlaps for polyatomic molecules includes not only the contributions of displacement parameters Δ calculated for the isolated vibrational modes but also the Dushinsky effect (mode mixing), as well as the changes of vibrational frequencies upon the electronic excitation. Although the very first algorithms for calculations of FC factors for polyatomic molecules within this approximation had been introduced in 1960s [45–47], their efficient implementations were developed much later, among them the implementation of the recursion relations derived by Doktorov et al. [48] for calculations of FC factors in Cartesian coordinates, presented by Gruner and Brumer [49] in late 80s along with the discussion of computational efficiency of many algorithms developed earlier at various level of sophistication. General recursion formulae and storing of the FC factors in the 2-D array were used by Ruhoff [50]. Later, Ruhoff and Ratner [51] presented an algorithm based on binary tree approach developed by Gruner and Brumer [49]. The Ruhof's approach to calculations of FC factors in Cartesian coordinates is readily applicable due to its efficiency and because most ab initio packages provide the normal modes represented in Cartesian atomic displacements.

In this study we use the general recursion formulae [48] for the calculation of the FC factors on the basis of Cartesian displacements of atoms in the molecule using the approach developed by Ruhoff [50] and implemented in the Scilab 4.0 [52] procedures [30] using over 4000 vibrationally excited configurations stored in the 2-D array. Our calculations are based on the simpler version of the general formulae relevant for the molecules cooled in supersonic-jet expansion (occupations of excited vibrational levels equal to zero in the ground electronic state) since no hot bands were identified in the LIF spectrum of AA [14,28]. The accuracy of this FC-fitting of geometry changes carried out in Cartesian coordinates [48,50] seems to be sufficient and the calculations of FC factors in the curvilinear internal coordinates (e.g. by means of the Dushin program of Reimers [53]) is unnecessary for the modeling of LIF spectrum of AA because of the following reasons. The changes of valence angles in the AA molecule seem to be considerable since they typically approach 5° (for skeletal angles in the aromatic system) and the largest change reaches 7.5° (C_2C_1N angle). Nevertheless, the errors of the FC-fitted geometry changes induced by the use of Cartesian coordinates do not depend on the total changes of valence angles upon the excitation. Importantly, the errors depend only on the differences between the values of valence angles used as the initial data for the FC calculations, which are computed via geometry optimization using some ab initio method and the final ones obtained via the FC fitting aided by vibrational analysis carried out with the same ab initio method. Actually, for the AA molecule the differences between these values are small and do not exceed 1° for the FC fitting aided by CC2 and 1.7° for the DFT-aided fit (for comparison see results of the FC fitting presented in Sections 5.1 and 6.1 and the relevant ab initio results [34]). The transformations needed for the FC fitting of the geometry changes are discussed in Sections 4.1–4.3 and the errors induced by the use of Cartesian coordinates instead of the internal curvilinear ones are discussed in Section 6.3.

We have considered only the geometry changes in normal coordinates of the in-plane modes and their influence on the LIF spectrum because essentially the AA molecule is planar in both electronic states. The equilibrium geometry of the molecule is planar in the S_1 state because of the strengthening of the π-electronic coupling between the nitrogen atom lone pair and the aromatic ring upon the excitation as well as the influence of the strong hydrogen bond between the amino group and the carboxylic group. Despite in the ground electronic state the equilibrium geometry of the amino group is non-planar, our studies of the barrier for the amino group inversion motion [33] proved that the AA molecule is effectively planarized in the lowest vibrational state due to the vibrational zero-point energy correction ZPE. The barrier height for the planar structure (obtained by extrapolation of the CC2 results to the CBS limit) is extremely low: 40–55 cm^{-1}, while the ZPE in the double well potential of the amino group inversion is roughly twice as high. Moreover, the deformation of the lowest vibrational wavefunction $\upsilon = 0$ for the amino group inversion due to the presence of the barrier is hardly discernible [33]. The computed barrier height is consistent with the experimentally determined isotopic shifts of the origin band in the LIF spectra (which are influenced by the ZPE) for the set of eight isotopologues of AA deuterated in various positions [31–33] in the substituent groups (NH_2,COOH, where H = ^{1}H or ^{2}H). Nevertheless, a few weak vibronic bands are assigned to overtones of the out-of-plane oscillations for the even vibrational quantum number (υ =2,4,...) or their combinations with other modes (usually in agreement with the earlier assignments [29]). The driving force of the presence of these bands in the excitation spectrum is not the geometry change since the molecule is planar and their displacement parameters are equal to zero. Among the possible factors which could cause of the presence of these bands in the spectrum the change of vibrational frequency upon the excitation or Fermi resonances, especially in the proximity of other stronger bands should be mentioned. Efficient vibronic coupling does not seem likely because the energies

of other electronic states are more than 1 eV higher. It should be emphasized that the FC fitting approach ought to be used as the way of refinement of the ab initio predicted geometry changes due to the fact even well resolved supersonic jet spectra facilitate the assignment of bands related to only a few normal modes (less than 10) but in large polyatomic molecules number of totally symmetric modes, whose intensities could carry the information concerning structural changes is often of order of a few dozens. Additionally, it is likely that weak bands present in congested ranges of the spectra are obscured, misinterpreted or involved in Fermi resonances and thus should not be used in the FC fitting.

4.1. Franck Condon modeling of LIF spectra

Previous investigations of the $S_0 \rightarrow S_1$ excitation of AA [28,30] indicated that the frequency changes and the Dushinsky effect have minor impact on the in-plane modes of frequencies below 900 cm^{-1}. These modes are responsible for the strong bands and progressions in the LIF spectrum of AA and facilitate evaluation of geometry changes upon the excitation. On the other hand strong mode mixing and noticeable changes of vibrational frequencies are predicted by ab initio methods for modes of frequencies 900–2000 cm^{-1}. In order to provide a clear insight into the influence of the geometry changes and other effects on band intensities we compare the advanced multidimensional model of FC factors (MFC) with the simple one-dimensional model (denoted as Δ-FC model). This approach is essentially the displaced harmonic oscillator model (DHO) based solely on reduced displacement parameters Δ_i for vibrational modes (ignoring the influence of frequency changes and the Dushinsky rotations), which provides simple algebraic equations for band intensities of overtones and combinations, thus facilitating the comprehensible discussion of accuracy of the estimated geometry change. In order to assure completeness of the modeled spectrum over 4000 vibrationally excited configurations were used in the modeling. This number included excitations up to at least $\upsilon = 2$ for all in plane modes and reaching of $\upsilon = 4$ for the in-plane modes of frequency below 900 cm^{-1} and up to $\upsilon = 6$ for the low-frequency modes of 253 cm^{-1} and 418 cm^{-1}.

In the Δ-FC model the relative intensity $I(\nu_i{}^{\upsilon}_{0})$ of the band (i.e., the band intensity divided by the intensity of the 0-0 transition) for the υth overtone of the ith vibration ν_i is given in the simplest form by equation Eq. (1)

$$I\left(\nu_i{}^{\upsilon}_{0}\right) = \frac{\Delta_i^{2\upsilon}}{\upsilon!} \tag{1}$$

where Δ_i is the form of the reduced displacement parameter for the ith vibration (ith normal coordinate) equal to the square root of the Huang-Rhys parameter (DHO model). The reduced displacement is related to the differences of equilibrium geometries for both electronic states as described in Section 4.3. In the Δ-FC model the intensities of combination bands are given by the product of the relevant expressions described by Eq. (1) for all vibrational modes contributing to the combination of interest. The Δ_i parameters are of fundamental importance and retain their physical meaning also within the MFC model, although their influence on band intensities is entangled in complicated recursion formulae [48–50] involving both the diagonal matrices comprising vibrational frequencies of the ground and the excited state and the Dushinsky matrix for the relevant electronic transition. The MFC model reduces to the Δ-FC model provided that the Dushinsky matrix is equal to unity and the vibrational frequencies remain unchanged upon the excitation.

The spectra modeled within MFC model and with both ab initio methods selected for this study are shown in Fig. 1. Only minor

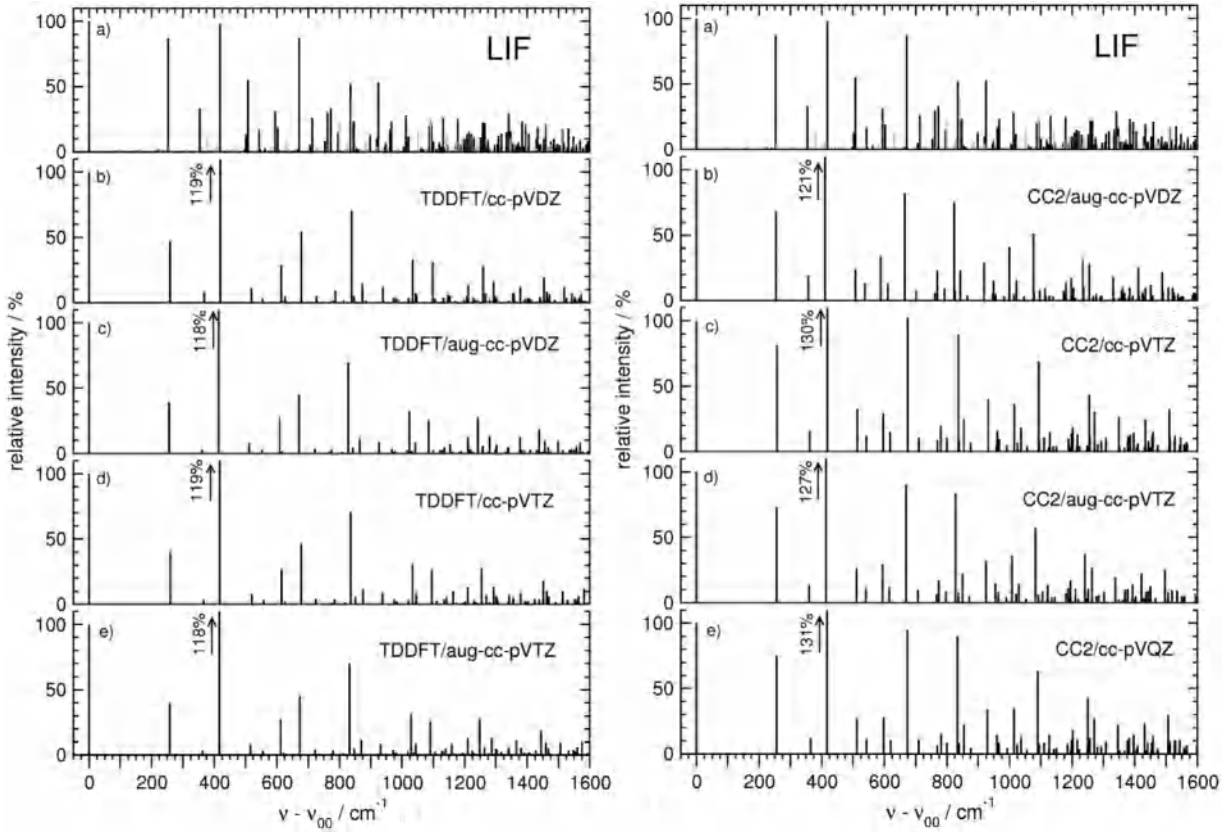

Fig. 1. Spectra modeled within the multidimensional F-C model using the TDDFT or CC2 results and the LIF spectrum (LIF bands assigned to out of plane modes or unassigned are printed in gray).

Table 1
Intensities of fundamentals in the excitation spectrum of anthranilic acid computed using multidimensional FC model with the approximate coupled-cluster CC2 and TD-DFT(B3LYP) results. Prominent bands are printed in bold and the vibrations forming long progressions are italic.

approximate coupled-cluster CC2						TD-DFT(B3LYP)				s-jet LIF		mode description
cc-pVTZ		aug-cc-pVTZ		cc-pVQZ		cc-pVTZ		aug-cc-pVTZ				
ν	I%	ν	I%	ν	I%	ν	I%	ν	I%	ν	I%	
257	**81**	**256**	**73**	**256**	**75**	**260**	**40**	**256**	**39**	*253*	*87*	*COOH rock.*
362	**16**	**360**	**14**	**364**	**12**	**366**	**4**	**360**	**5**	**354**	**33**	**NH_2 rock.**
418	**130**	**414**	**127**	**417**	**131**	**418**	**119**	**413**	**118**	*418*	*98*	*H ring defor.*
543	12	541	12	543	11	558	3	557	3	543	17	ring defor. 6a
597	**29**	**594**	**29**	**598**	**28**	**615**	**27**	**611**	**26**	**595**	**31**	**OCO scissor., ring bend.**
710	**11**	**708**	**10**	**710**	**11**	**724**	**4**	**719**	**5**	**713**	**26**	**ring CC str 1, C_2C_7 str**
838	**9**	**837**	**8**	**839**	**9**	**851**	**6**	**848**	**7**	**841**	**22**	**ring defor. 12**
991	5	990	4	992	5	1020	3	1016	3			CC ring str.
1025	7	1021	7	1025	7	1045	9	1049	8			CC ring str.
1125	3	1120	3	1125	3	1135	3	1130	3			HNH rock., (CH bend.)
1150	5	1144	4	1149	5	1164	10	1165	11	1119	7	CH bend. (CC str.)
1201	18	1195	17	1202	18	1210	13	1208	12	1230	11	OH bend, (C_2C_7 str, CH bend)
1308	11	1302	8	1308	9	1301	7	1306	7			CN str, (CC str, CH bend)
1334	1	1324	5	1333	3	1342	7	1335	7			C–O str, CC str
1397	**14**	**1392**	**14**	**1397**	**15**	**1379**	**9**	**1378**	**8**	**1395**	**21**	**CC str, CH bend**
1432	3	1429	4	1434	3	1450	2	1444	1			CC str, CH bend
1527	9	1518	8	1529	10	1555	0	1547	0			CC str
1604	7	1593	7	1599	7	1564	6	1579	6			NH_2 scissor
1693	6	1678	6	1686	6	1685	6	1668	6			C=O str

(a few percent) discrepancies of band intensities appear between both models of FC factors and among the spectra modeled with the same quantum chemistry method; also choice of the basis set brings about little changes to the results. The above indicates that the influence of the Dushinsky effect on the AA spectrum is very limited. Significant discrepancies appear only when the spectra modeled on the basis of TDDFT and CC2 are compared with each other or with the experimental one. Mainly two long progressions build on frequencies 253 cm^{-1} and 418 cm^{-1} as well as combinations of their overtones with other fundamentals generate a quite rich vibronic structure, which includes many moderate- and low-intensity bands. The spectral congestion generated in this way increases gradually starting from roughly 500 cm^{-1} above the origin band and becomes significant in the range above 1000 cm^{-1}. The TDDFT spectra are the most contrasting with the experimental one since the TDDFT band intensities for fundamentals are significantly underestimated (except for the 418 cm^{-1} band, as well as its overtones and combinations), which makes the intensities of overtones underestimated even more severely. The CC2 results show significantly better agreement with the experimental band intensities for the fundamental bands. Also, the overall distribution of intensities in the whole spectra is noticeably better.

The intensities of fundamental bands calculated using the MFC model with the TDDFT and CC2 methods are shown in Table 1. For almost all the fundamental bands of substantial intensities in the experimental spectrum (bold data in Table 1) the DFT&TDDFT results are significantly underestimated, with only two exceptions: the intensity band 418 cm^{-1} is overshoot by ca. 20% and the intensity of the band 595 cm^{-1} is predicted almost accurately. The CC2 method yields significantly improved results for many fundamentals, among them (which is especially important) almost perfect intensity for the band 253 cm^{-1} that generates a long progression throughout the whole spectrum. Nevertheless, even the CC2 results leave some room for improvement.

For the middle-frequency modes (900–2000 cm^{-1}) the FC calculations based on the CC2 results predict the presence of only two moderate intensity bands (assigned to the LIF bands 1230 cm^{-1} and 1395 cm^{-1} (the later one is unusually broad 2.4 cm^{-1} probably as the result of blending of a few bands) and their intensities based on the TDDFT results are noticeably smaller. FC modeling predict negligible intensities for all high-frequency stretching modes involving hydrogen atoms. Even for the N–H_{bond} stretch the reduced displacement parameter is very small, despite the noticeable H atom dislocation along the hydrogen bond. This is because the H atom dislocation involves the motion of only one atom light atom. It is in contrast with the activity of the skeleton modes, for which geometric displacements of quite a few heavier atoms (C, N, O) weighted by the square root of atomic masses easily generate medium-intensity bands. The calculated intensity of the N–H_{bond} stretching mode predicted on the basis of ab initio results is below 2% of the origin band intensity. This is the essential dissimilarity with the salicylic acid molecule, for which the displacement parameter Δ for the phenolic O–H_{bond} stretching mode is larger than 1 [18,27], so the corresponding fundamental and its overtones are essential for the presence of the dual fluorescence band [18].

4.2. Fitting of displacement parameters according to experimental LIF intensities

The computed displacement parameters can be adjusted to give better agreement with the experimental band intensities and yield more reliable estimation of the changes of the equilibrium geometry upon the excitation. Fig. 2 shows the LIF spectrum alongside the spectra modeled on the basis of the LIF intensities for the selected bands and the CC2 or TDDFT(B3LYP) normal modes, denoted below as LIF+CC2 FC fit and LIF+TDDFT FC fit, respectively.

The bands selected for the fitting are marked with circles. The choice of a reliable set of the experimental band intensities and the relevant set of displacement parameters is essential for the FC fitting. The selected bands should be well separated from other ones, their shape and bandwidth should be similar to other bands in the LIF spectrum, and they should have a convincing, unequivocal assignment. The displacement parameters should be optimized for only those vibrational modes, for which at least a few overtones or combination bands fulfill the above requirements, thus providing sufficient experimental base for the fitting procedure. The experimental data allowed for identification of 10 in-plane modes active in the LIF spectrum of AA [28], though only seven of them generate substantial amount of strong or medium intensity bands that

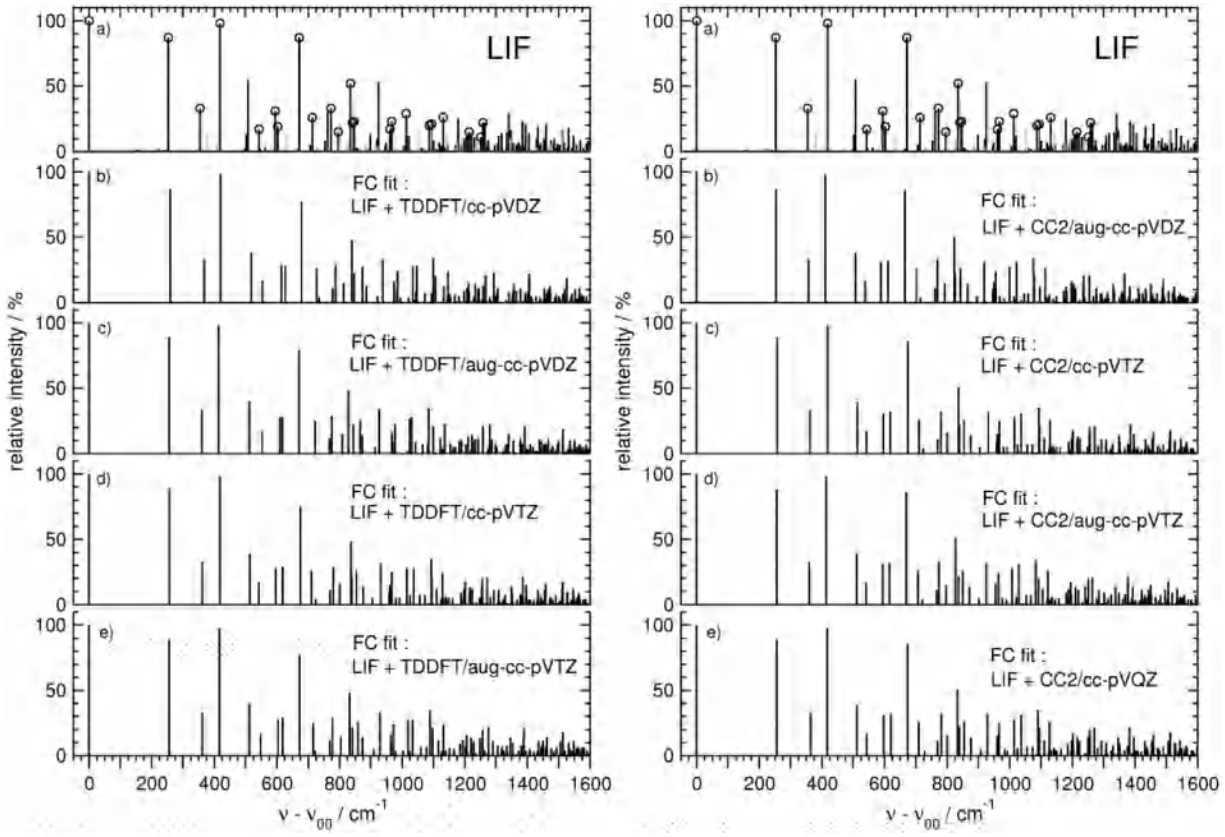

Fig. 2. The FC-fitted spectra modeled on the basis of the LIF intensities for the bands marked with circles and the CC2 or TDDFT(B3LYP) normal modes. LIF bands assigned to out-of-plane modes or unassigned are printed in gray.

are relevant for the fitting. Eventually, the displacement parameters for the seven modes (LIF: 253 cm^{-1}, 354, 418, 543, 595, 713 and 841 cm^{-1}) were chosen for optimization concerning 22 most prominent vibronic bands. Other parameters were kept frozen at values resulting directly from the ab initio calculations.

The optimization of the Δ_i parameters was based on the least square method from the Scilab4.0[52] package and build-in OPTIM procedure. The cost function given by Eq. (2) used in minimization procedure is the standard deviation of the fitted intensities based on the RMS of the differences between the experimental and the fitted intensities for the $N=22$ selected vibronic bands (marked with circles in Fig. 2).

$$S_I = \sqrt{\frac{1}{N}\sum_{i=1}^{N}\left(I_i^{FC} - I_i^{LIF}\right)^2} \tag{2}$$

Before the FC fitting the overall standard deviation of the computed CC2 intensities is about 18 (in arbitrary units of intensity, for which I_{00} is normalized to 100), while the deviation of the TDDFT intensities is about 26. This is related to the underestimated ab initio computed intensities, which are significantly smaller for TDDFT then for CC2 (see Fig. 1 and Table 1). During the fitting the value of the cost function decreased roughly three times for LIF+CC2 FC fitting and as much four times for LIF+TDDFT FC fitting. The above makes the standard deviation of the final FC fitt about 6 units for both CC2-aided and the TDDFT-aided FC fitting, these values are only about 0.3 (5%) larger for the later than for the former ones. The standard deviations for the FC fits are comparable with the errors of experimental intensities of roughly $0.05 \times I_{00}$. Only minor variations of the standard deviation are observed due to the use of various basis used in ab initio calculations (about 6–7% of their values) and due for the use of the MFC model or the Δ-FC model(about 3%). So small discrepancy between these two models is achieved owing to two issues. Firstly, owing to quite small Dushinsky effect for the modes that generate the prominent vibronic bands in the spectrum and included in the FC fitting. Despite strong mode mixing is predicted by ab initio calculations for the modes of frequencies 1000–1800 cm^{-1}, these modes generate only a few minor vibronic features, which are not included in the FC fitting. Secondly, only the vibronic bands that involve transitions for rather low values of vibrational quantum numbers were included in the fitting since the main aim of this work is reliable estimation of geometry changes possibly not influenced by other effects, which are enhanced for higher vibrational quantum numbers or for higher density of vibronic states. Both above reasons provide little opportunity for the manifestation of discrepancies between the FC models.

4.3. Inverse Franck–Condon modeling of geometry changes

The vector of geometry of geometry changes $\vec{D}$ can be calculated from the differences of mass-weighted coordinates $\xi_k = x_k\sqrt{m_k}$ for the relevant equilibrium geometries or directly from the differences of Cartesian equilibrium geometries multiplied by the squares of masses for the relevant atoms, according to Eq. (3):

$$\mathbf{D}_{ex}^{MW} = \mathbf{L}_{ex}^{MW,T}\left(\vec{\xi}_{ex}^{eq} - \vec{\xi}_{gr}^{eq}\right) = \mathbf{L}_{ex}^{MW,T}M^{1/2}\left(\vec{x}_{ex}^{eq} - \vec{x}_{gr}^{eq}\right) \tag{3}$$

where $\mathbf{M}$ is the diagonal matrix of atomic masses of size $3\,N \times 3\,N$. The $\vec{D}$ vector is needed for calculation of the reduced displacement parameters Δ_i, crucial for evaluation of the FC factors. The reduced displacement parameter Δ_i for the ith mode can be calculated form the relevant mass-weighted displacements $\mathbf{D}_{ex\,i}^{MW}$

according to Eq. (4), where ν_i is the vibrational frequency of the mode given in cm^{-1}.

$$\Delta_i = \sqrt{\frac{2\pi^2\nu_i}{hc}} D^{MW}_{ex,\,i} = \sqrt{\frac{2\pi^2\mu_i\nu_i}{hc}} D^{Cart}_{ex,\,i} \quad (4)$$

The above definition of the reduced displacement differs from the standard reduced displacement parameter by factor $2^{½}$ but it is directly related to Huang-Rhys parameter (DHO model) with makes the form of Eq. (1) particularly simple. Since the square root of the reduced mass is included in the definition of mass-weighted displacements, when the properly normalized Cartesian displacements $D^{Cart}_{ex\,i}$ are used, the square root of the reduced mass and vibrational frequency $\sqrt{\mu_i\nu_i}$ appears (alternatively, the factor $\sqrt[4]{\mu_i k_i}$ can be used, which usually appears in the quantum harmonic oscillator theory). Note that the vibrational structure of LIF spectra and absorption spectra are associated with vibronic activity of the molecules in their excited states.

When the optimized values of Δ_i parameters are already known, the values of $\mathbf{D}^{MW}_{ex\,i}$ can be calculated easily transforming Eq. (4). Then the differences of Cartesian equilibrium coordinates can be calculated inverting matrix relation Eq. (3) which leads to Eq. (5).

$$\Delta\bar{x}^{eq} = \bar{x}^{eq}_{ex} - \bar{x}^{eq}_{gr} = \mathbf{L}^{MW}_{ex} M^{-1/2} \mathbf{D}^{MW}_{ex} \quad (5)$$

5. Structural implications and discussion

5.1. Structural changes upon electronic excitation

The FC-fitted geometry changes calculated on the basis of CC2 and TDDFT(B3LYP) vibrational analysis are qualitatively consistent, though they show some residual differences. For the sake of consistency let us compare the FC-fitted geometry changes calculated with the aid of CC2 (shown in Fig. 3) and TDDFT results (Fig. 4) computed using the same high-quality basis set aug-cc-pVTZ and the same model of FC factors (MFC).

The essential changes of geometry parameters evaluated via the FC-fitting are significantly larger than differences between the *ab initio* optimized geometries for both electronic states. The above concurs with the fact that the theoretically computed intensities of the vibronic bands calculated on the basis of the *ab initio* optimized geometries are significantly smaller than their experimental counterparts. This issue is especially evident for the geometry parameters that concern the intramolecular hydrogen bond.

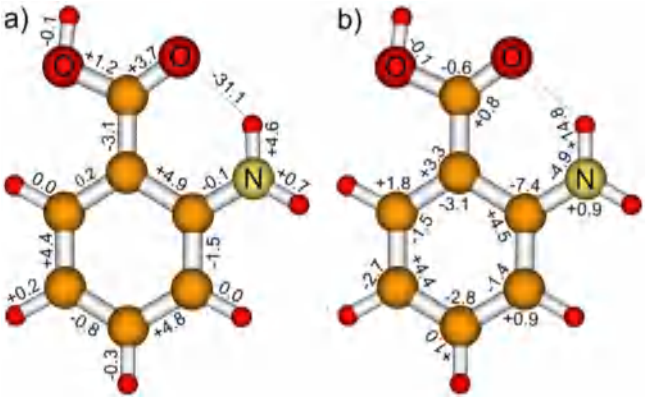

Fig. 3. Changes of the equilibrium geometry parameters for anthranilic acid upon the $S_0 \rightarrow S_1$ excitation obtained using the multidimensional F-C (MFC) fitting procedure with the aid of the CC2/aug-cc-pVTZ vibrational analysis: a) bond lengths /pm, b) valence angles in degrees.

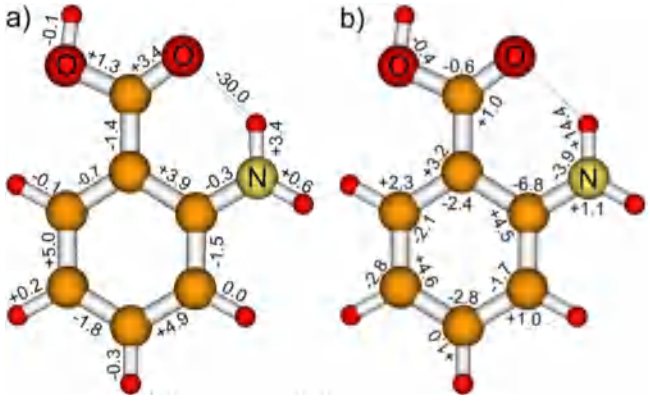

Fig. 4. Changes of the equilibrium geometry parameters for anthranilic acid upon the $S_0 \rightarrow S_1$ excitation obtained using the multidimensional F-C (MFC) fitting procedure with the aid of the TDDFT(B3LYP)/aug-cc-pVTZ vibrational analysis: a) bond lengths /pm, b) valence angles in degrees.

Generally, the changes of equilibrium geometry evaluated with the LIF+CC2 FC-fitting are noticeably larger than values estimated with the LIF+TDDFT FC-fitting, especially for the H-chelate ring. Although discrepancies between these estimates are much smaller than those between the results of *ab initio* geometry optimization computed with CC2 and TDDFT methods [34] they retain some residual features of the ab initio computed geometry changes. Because the CC2 ab initio geometry changes are much closer to the results of the FC fittings than the TDDFT ones and the corrections imposed by the FC fitting on the CC2 geometry changes are relatively small, the geometry changes calculated with the LIF+CC2 FC-fitting can be regarded as more reliable and accurate than the LIF+TDDFT FC-fitting ones.

The estimated shortening of the H···O distance (−31.1 pm according to LIF+CC2 FC-fit and −30.0 pm with the LIF+TDDFT FC-fit) are quantitatively consistent (with accuracy ca.1 pm). Although the remaining discrepancy between these values is not negligible, it is much smaller than the discrepancy between the *ab initio* CC2 and DFT-computed geometry changes, which are equal to −27.3 pm and −19.1 pm [34], respectively. According to the LIF+CC2 fit the N–H_{bond} bond is longer by 4.6 pm than in the ground state. The shortening of the hydrogen bond is facilitated mainly by deformations of the valence angles. The largest deformation concerns the C_2–C_1–N angle, which decreases by 7.4°.

The excitation to the $S_1(\pi\pi^*)$ state induces moderate changes of the bond alternation in the π-electronic system of AA. These changes are the largest for the aromatic ring, in which the C_1–C_2, C_3–C_4 and C_5–C_6 bonds becomes longer by roughly 4–5 pm. The magnitude of the changes of bond alternation in the carboxylic group is slightly smaller. The increase of the C=O bond length by +3.7 pm (LIF+CC2 FC-fit) indicate the weakening of this bond typical for the carbonyl group involved in the hydrogen bond formation. This is accompanied by the largest shortening of the valence bond in the AA molecule (−3.1 pm) which concerns the C_2–C_7 bond linking the COOH group with the aromatic ring. These geometry changes indicate an increase of π-electronic coupling between the carboxylic group and the benzene ring that is related with significant aromatization of this group in the excited state.

5.2. Excited-state geometry

The geometry parameters for the S_1 excited state can be evaluated using the LIF+ CC2 FC-fitted geometry change upon the $S_0 \rightarrow S_1$ excitation (preferably with the multidimensional MFC model) in combination with some well-established ground state

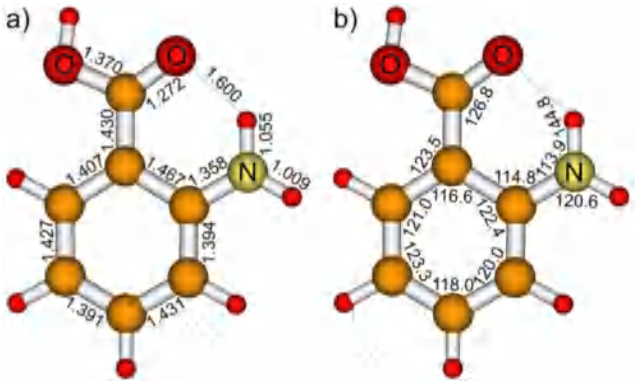

Fig. 5. The S_1 excited-state geometry of anthranilic acid evaluated form the CC2/cc-pVQZ ground-state geometry and the F-C fitted geometry changes upon the $S_0 \rightarrow S_1$ excitation: a) bond lengths /Å, b) valence angles in degrees.

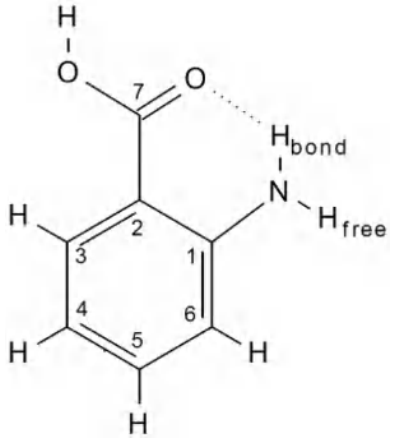

Fig. 6. Atom numbering used for the anthranilic acid molecule in this work.

geometry (e.g. CC2/cc-pVQZ) [34]. The resulting geometry parameters are presented in Fig. 5, and the atom numbering in the AA molecule is shown in Fig. 6. These results imply that the O···H distance is equal to 1.60 Å, which is significantly shorter than 1.638 Å computed with CC2/cc-pVQZ and indicate formation of strong hydrogen bond in the S_1 state.

The dislocation of the H atom along the N–H···O bridge makes the $N–H_{bond}$ bond longer than the $N–H_{free}$ by 4.6 pm. The strengthening of the hydrogen bond causes substantial distortions of valence angles within the amino group and makes it significantly asymmetric. The C–N–H angles differ by 6.7° and both C–C–N angles differ by 8°.

The pattern of bond alternation in the π-electronic system yield by the LIF+CC2 FC-fitting is similar to the results of the CC2 ab initio calculation but the lengthening of valence bonds is noticeably larger in the former one. The length of the $C_1–C_2$ bond, which is significantly larger than other bonds in the aromatic ring already in the ground state, in the excited state increases further to reach 1.467 Å (substantially more than 1.458 Å computed with CC2/cc-pVQZ). In contrast to the above, the $C_2–C_7$ bond (linking the carboxylic group with the aromatic ring) which in the ground state is almost a single bond, in the excited state becomes as strong as the bonds in the aromatic ring and its length decreases to 1.430 Å. This pattern of bond alternation can be rationalized assuming that the predominant resonance structure for the S_1 excited state has the single $C_1–C_2$ bond and strong π-electronic coupling of the carboxyl group with the benzene ring.

6. Reliability and accuracy of the estimated geometry changes

6.1. Discrepancies caused by the use of different ab initio methods

The changes in the length of the O···H distance estimated via FC fitting within the Δ-FC and the MFC models and aided by the CC2 or TDDFT vibrations with a series of basis sets are depicted in Fig. 7 along with the ab initio values computed with the above quantum chemistry methds [34]. The values of the shortening of the H···O distance computed with the aid of the CC2 vibrations are scattered in the range from −30.3 to −31.6 pm (the variations are noticeable but they are small in relative terms). The values evaluated with the LIF+TDDFT approach are roughly 1 pm smaller than the LIF+CC2 ones and are dispersed in the range from −29.3 to −30.6 pm. The estimates obtained with the largest basis sets: LIF+CC2/cc-pVQZ MFC fit equals to −31.2 pm and LIF+TDDFT MFC fit equals to −30.0 pm. The residual discrepancy (roughly 1pm) resulting from the use of CC2 or TDDFT vibrations is comparable with other errors, which includes the errors due to the use of different basis sets in vibrational analysis, or the use of the Δ-FC and the MFC models as well as the errors due to inaccuracy of experimental band intensities (Section 6.2).

Variations of the differences of geometry parameters (between the S_0 and S_1 state) obtained with a series of basis sets using the LIF+CC2 FC fitting are shown in Table 2. The largest changes in bond lengths (of magnitude 4–5 pm) are scattered over 0.3 pm at the most. The discrepancies of the changes of valence angles do not exceed 0.3°. In contrast to the *ab intio* CC2 results [34] the LIF+CC2 FC-fits do not reveal any clear basis set dependence.

Variations of the changes of geometry parameters caused by the use of a series of correlation-consistent basis sets in the LIF+TDDFT FC fitting, presented in Table 3 are similar in magnitude to the LIF+CC2 results (cf. Table 2). Nevertheless, the values calculated with the LIF+TDDFT FC fitting are noticeably smaller than the

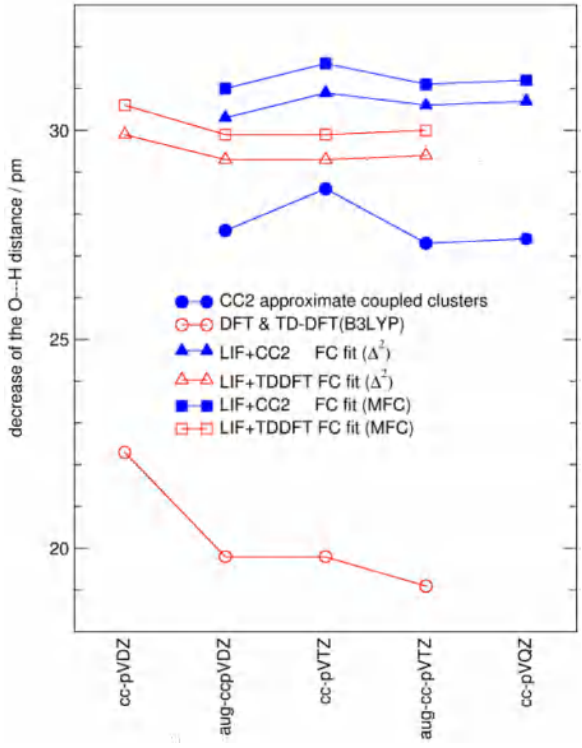

Fig. 7. Changes in the length of the O•••H distance estimated via FC fitting and *ab initio* methods.

Table 2
Changes of equilibrium geometry parameters acid upon the $S_0 \rightarrow S_1$ excitation fitted using the basic model dependent solely on the square of the reduced displacement Δ^2 and multidimensional FC (MFC) with the aid of the CC2 vibrational analysis.

approach:			fitting of FC factors: LIF spectrum + CC2 vibrations								LIF+DFT[30]	ab initio CC2[34]	
basis set: FC model:			cc-pVTZ		cc-pVQZ		aug-cc-pVDZ		aug-cc-pVTZ		cc-pVDZ	aug-cc- pVTZ	cc-pVQZ
			Δ[2]	MFC	Δ[2]	MFC	Δ[2]	MFC	Δ[2]	MFC	MFC		
Δ*R*(A–B) / pm	aromatic ring	**C_1–C_2**	**4.7**	**4.8**	**4.8**	**4.9**	**4.9**	**4.9**	**4.8**	**4.9**	**4.0**	**3.9**	**3.9**
		C_3–C_4	**4.5**	**4.5**	**4.5**	**4.5**	**4.3**	**4.3**	**4.4**	**4.4**	**4.9**	**4.4**	**4.4**
		C_4–C_5	−0.8	−0.8	−0.8	−0.8	−0.8	−0.8	−0.8	−0.8	−1.7	−1.0	−1.0
		C_5–C_6	**4.9**	**5.0**	**4.9**	**4.9**	**4.6**	**4.6**	**4.8**	**4.8**	**5.1**	**4.5**	**4.6**
		C_1–C_6	−1.6	−1.6	−1.5	−1.5	−1.4	−1.4	−1.5	−1.5	−1.0	−1.7	−1.7
	substituents	C_1–N	0.1	0.2	0.1	0.1	0.0	0.1	0.1	0.1	1.7	−0.6	−0.5
		N–H_{free}	0.8	0.8	0.7	0.7	0.7	0.7	0.7	0.7	0.8	0.7	0.7
		N–H_{bond}	**4.8**	**4.8**	**4.7**	**4.7**	**4.2**	**4.3**	**4.6**	**4.6**	**3.7**	**4.3**	**4.3**
		C_2–C_7	**−3.1**	**−3.3**	**−3.0**	**−3.1**	**−2.8**	**−2.8**	**−3.0**	**−3.1**	−1.0	**−3.0**	**−3.1**
		C_7=O	**3.7**	**3.7**	**3.7**	**3.7**	**3.8**	**3.8**	**3.7**	**3.7**	**3.3**	**3.7**	**3.7**
		C_7–O	1.3	1.2	1.2	1.2	1.2	1.1	1.2	1.2	1.7	1.2	1.2
		O···H	**−30.9**	**−31.6**	**−30.7**	**−31.2**	**−30.3**	**−31.0**	**−30.6**	**−31.1**	**−30.2**	**−27.3**	**−27.4**
		O·····N	**−13.4**	**−14.0**	**−13.4**	**−13.8**	**−13.2**	**−13.7**	**−13.2**	**−13.8**	**−11.6**	**−10.5**	**−10.7**
angles / degrees	aromatic ring	**C_2–C_1–C_6**	**4.6**	**4.5**	**4.5**	**4.5**	**4.5**	**4.4**	**4.5**	**4.5**	**4.2**	**4.8**	**4.9**
		C_1–C_2–C_3	**−3.3**	**−3.1**	**−3.2**	**−3.2**	**−3.1**	**−3.0**	**−3.1**	**−3.1**	**−2.6**	**−4.1**	**−4.1**
		C_3–C_4–C_5	**4.3**	**4.4**	**4.4**	**4.4**	**4.4**	**4.5**	**4.4**	**4.4**	**4.9**	**3.6**	**3.7**
		C_4–C_5–C_6	**−2.9**	**−2.9**	**−2.8**	**−2.8**	**−2.7**	**−2.8**	**−2.8**	**−2.8**	**−2.7**	**−3.1**	**−3.2**
		C_1–C_6–C_5	−1.4	−1.3	−1.4	−1.3	−1.4	−1.4	−1.4	−1.4	−2.0	−0.9	−1.0
	substituents	**C_2–C_1–N**	**−7.5**	**−7.4**	**−7.5**	**−7.4**	**−7.3**	**−7.4**	**−7.5**	**−7.4**	**−7.2**	**−7.2**	**−7.3**
		C–N–H_{free}	0.9	0.9	0.9	0.9	1.0	1.0	0.9	0.9	1.1	1.0	0.9
		C–N–H_{bond}	**−4.9**	**−5.0**	**−4.9**	**−4.9**	**−4.7**	**−4.8**	**−4.9**	**−4.9**	**−4.0**	**−4.5**	**−4.5**
		C_3–C_2–C_7	**3.2**	**3.2**	**3.2**	**3.3**	**3.2**	**3.3**	**3.3**	**3.3**	**2.4**	**3.5**	**3.4**
		C_2–C_7=O	0.8	0.7	0.8	0.8	0.9	0.9	0.8	0.8	0.9	1.3	1.3
		N–H···O	**15.0**	**15.0**	**14.8**	**14.9**	**14.7**	**14.8**	**14.8**	**14.8**	**14.9**	**14.5**	**14.4**
		C=O···H	**−3.7**	**−3.4**	**−3.6**	**−3.5**	**−3.6**	**−3.5**	**−3.6**	**−3.5**	**−4.9**	**−4.8**	**−4.7**

Table 3
Changes of equilibrium geometry parameters acid upon the $S_0 \rightarrow S_1$ excitation fitted using the basic model dependent solely on the square of the reduced displacement Δ^2 and the multidimensional F-C factors (MFC) with the aid of the DFT(B3LYP) and TDDFT vibrational analysis.

		approach:	fitting of FC factors: LIF spectrum + TDDFT(B3LYP) vibrations									TDDFT[34]
		basis set:	cc-pVDZ		cc-pVTZ		aug-cc-pVDZ		aug-cc-pVTZ		cc-pVDZ[30]	aug-cc-pVTZ
		FC model:	Δ[2]	MFC	Δ[2]	MFC	Δ[2]	MFC	Δ[2]	MFC	MFC	
Δ*R*(A–B) / pm	aromatic ring	**C_1–C_2**	**3.7**	**3.7**	**3.7**	**3.8**	**3.6**	**3.7**	**3.8**	**3.9**	**4.0**	**2.3**
		C_3–C_4	**4.7**	**4.8**	**5.0**	**5.0**	**4.9**	**4.9**	**5.0**	**5.0**	**4.9**	**4.9**
		C_4–C_5	−1.6	−1.6	−1.8	−1.8	−1.7	−1.7	−1.8	−1.8	−1.7	−2.1
		C_5–C_6	**4.9**	**5.0**	**4.9**	**4.9**	**4.7**	**4.7**	**4.9**	**4.9**	**5.1**	**4.3**
		C_1–C_6	−0.7	−1.0	−1.6	−1.5	−1.4	−1.4	−1.5	−1.5	−1.0	−1.7
	ubstituents	C_1–N	1.4	1.5	0.8	0.9	0.0	0.0	−0.3	−0.3	1.7	−0.1
		N–H_{free}	0.7	0.7	0.5	0.5	0.5	0.5	0.6	0.6	0.8	0.4
		N–H_{bond}	**3.5**	**3.5**	**3.3**	**3.4**	**3.5**	**3.4**	**3.4**	**3.4**	**3.7**	**2.5**
		C_2–C_7	**−1.4**	**−1.4**	**−1.3**	**−1.4**	**−1.3**	**−1.4**	**−1.3**	**−1.4**	**−1.0**	**−1.3**
		C_7=O	**3.2**	**3.2**	**3.4**	**3.4**	**3.3**	**3.4**	**3.4**	**3.4**	**3.3**	**3.2**
		C_7–O	1.4	1.4	1.3	1.3	1.4	1.4	1.3	1.3	1.7	1.2
		O···H	**−29.9**	**−30.6**	**−29.3**	**−29.9**	**−29.3**	**−29.9**	**−29.4**	**−30.0**	**−30.2**	**−19.1**
		O·····N	**−13.0**	**−12.8**	**−12.7**	**−12.9**	**−12.8**	**−13.0**	**−12.8**	**−13.0**	**−11.6**	**−6.5**
angles / degrees	aromatic ring	**C_2–C_1–C_6**	**4.6**	**4.7**	**4.5**	**4.5**	**4.4**	**4.5**	**4.5**	**4.5**	**4.2**	**4.0**
		C_1–C_2–C_3	**−2.4**	**−2.5**	**−2.4**	**−2.4**	**−2.5**	**−2.4**	**−2.5**	**−2.5**	**−2.6**	**−3.5**
		C_3–C_4–C_5	**4.6**	**4.7**	**4.5**	**4.6**	**4.5**	**4.6**	**4.5**	**4.6**	**4.9**	**2.9**
		C_4–C_5–C_6	**−2.7**	**−2.6**	**−2.7**	**−2.8**	**−2.7**	**−2.8**	**−2.7**	**−2.8**	**−2.7**	**−3.0**
		C_1–C_6–C_5	−1.8	−1.9	−1.7	−1.7	−1.7	−1.7	−1.7	−1.7	−2.0	−0.5
	substituents	**C_2–C_1–N**	**−6.7**	**−6.8**	**−6.7**	**−6.7**	**−6.5**	**−6.7**	**−6.7**	**−6.8**	**−7.2**	**−5.7**
		C–N–H_{free}	1.1	1.1	1.0	1.1	1.0	1.0	1.1	1.1	1.1	1.0
		C–N–H_{bond}	**−3.9**	**−3.8**	**−3.8**	**−3.8**	**−3.7**	**−3.8**	**−3.9**	**−3.9**	**−4.0**	**−3.2**
		C_3–C_2–C_7	**3.0**	**3.1**	**3.2**	**3.2**	**3.1**	**3.1**	**3.2**	**3.2**	**2.4**	**2.7**
		C_2–C_7=O	1.0	1.0	1.0	1.0	0.0	0.0	1.0	1.0	0.9	1.6
		N–H···O	**14.3**	**14.4**	**14.1**	**14.3**	**14.2**	**14.2**	**14.1**	**14.4**	**14.9**	**11.0**
		C=O···H	**−3.6**	**−3.7**	**−3.3**	**−3.5**	**−3.4**	**−3.5**	**−3.3**	**−3.4**	**−4.9**	**−4.3**

former ones. The changes in length of the C_1–C_2 bond are ca. 1 pm smaller than the LIF+CC2 ones and the hydrogen atom dislocation is smaller by roughly 1.5 pm. Noticeably, the shortening of the C_2–C_7 bond estimated with the LIF+TDDFT fitting is by almost 2 pm smaller than with the LIF+CC2 fitting. Also, the most pronounced changes of valence angles (especially in the amino group) are smaller by 0.5°–1.0°. These discernible systematic differences between the results of LIF+CC2 and the LIF+TDDFT approaches indicate that the latter noticeably underestimates the magnitude of the pseudoaromatic conjugation in the H-chelate ring, which is the important factor that causes the strengthening of the intramolucular hydrogen bond in the π-conjugated molecules [24-27].

6.2. Contributions of selected vibrations to the fitted geometry change

A comprehensible insight into the contributions of selected vibrations to the evaluated geometry changes can be gained by analyzing the dependence of the intensities of fundamental bands on the displacement parameters in the simple model of displaced harmonic oscillator (Δ-FC model). Substitution of Eq. (4) into Eq. (1) gives for the change of the vibrational quantum number $\upsilon = 0 \rightarrow 1$ the intensities of the fundamental bands, which are equal to the squares of the reduced displacement parameters. They, in turn, are related to the squares of the mass-weighted displacements multiplied by the vibrational frequencies, or to the squares of the Cartesian displacements $D^{\mathrm{Cart}}_{\mathrm{ex}\ i}$ multiplied by the frequencies and the reduced masses, as shown in Eq. (6):

$$I\left(\nu_{i\,0}^{\ 1}\right) = \Delta_i^2 = \frac{2\pi^2}{hc}\nu_i D^{\mathrm{MW}\,2}_{\mathrm{ex},\ i} = \frac{2\pi^2}{hc}\mu_i\nu_i D^{\mathrm{Cart}\,2}_{\mathrm{ex},\ i} \tag{6}$$

The factor $\mu_i\nu_i$ amplifies the impact of high-frequency vibrations and heavy oscillators on the LIF spectrum. The predominant effect increases the intensities of fundamentals proportionally to their frequencies, which vary from roughly 250 cm^{-1} to more than 3500 cm^{-1} for AA. This is accompanied by somewhat smaller decrease of the reduced masses of the oscillators from about 4–7 a.m.u. for frequencies below 900 cm^{-1} to values hardly exceeding 1 a.m.u. for high frequency stretching modes (as they involve mostly the motion of hydrogen atoms).

Transformation of Eq. (6) facilitates evaluation of the absolute value of Cartesian displacement parameters, on the basis of the experimental intensities shown in Eq. (7).

$$\left|D^{\mathrm{Cart}}_{\mathrm{ex}\ i}\right| = \sqrt{\frac{hc}{2\pi^2}\frac{I\left(\nu_{i\,0}^{\ 1}\right)}{\mu_i\nu_i}} \tag{7}$$

Because of the square root present in the above equation, this implies that the relative errors of Cartesian displacements due to experimental uncertainties are equal to half of the relative errors of the experimental band intensities for the fundamentals and should not exceed 2,5% of the magnitude of geometry changes.

The importance of vibrational modes taken into account in the fitting of Frack–Condon factors for the total geometry changes can be evaluated by dividing the sum of squares of the selected Cartesian displacements by the sum of squares of all Cartesian displacements (31 parameters for all totally symmetric modes). Alternatively, the intensities of the relevant fundamentals divided by their frequencies and the reduced masses can be summed, as shown in Eq. (8). Such contributions are additive and can be normalized to unity. This equation represents the square of the length of the vector consisting of displacement parameters that were optimized by FC fitting, divided by the square of the length of the vector representing the total geometry change.

$$\frac{\left\|\vec{D}^{\mathrm{Cart}}_{\mathrm{ex\,FCfit}}\right\|^2}{\left\|\vec{D}^{\mathrm{Cart}}_{\mathrm{ex\ Total}}\right\|^2} = \frac{\sum\limits_{i=FC\,fit}\left(D^{\mathrm{Cart}}_{\mathrm{ex}\ i}\right)^2}{\sum\limits_{j}\left(D^{\mathrm{Cart}}_{\mathrm{ex}\ j}\right)^2} = \frac{\sum\limits_{i=FC\,fit}\frac{I\left(\nu_{i\,0}^{\ 1}\right)}{\mu_i\nu_i}}{\sum\limits_{j}\frac{I\left(\nu_{j\,0}^{\ 1}\right)}{\mu_j\nu_j}} \tag{8}$$

The contributions of the in-plane modes to the sum of intensities of all fundamentals (equal to the to the sum of squares of the reduced displacements Δ_i) and the contributions of the sum of these intensities weighted by factor $1/\mu_i\nu_i$ (equal to the sum of squares of the Cartesian displacements $D^{\mathrm{Cart}}_{\mathrm{ex}\ i}$) are compared in Fig. 8.

The influence of the weighting by factor $1/\mu_i\nu_i$ implies that the contributions of low-frequency fundamentals to the FC-fitted geometry changes are larger than their contributions to the sum of intensities in the spectrum, while typically for the fundamentals of frequencies higher than roughly 500 cm^{-1} the opposite effect is present. The seven displacement parameters optimized in

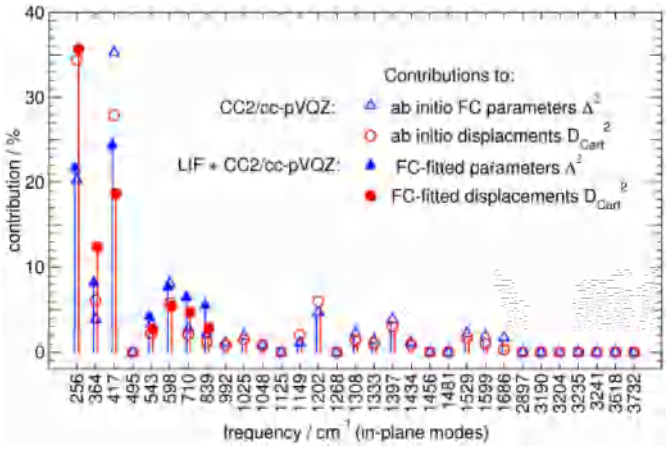

Fig. 8. Contributions of the squares of the reduced displacements Δ_i and the squares of Cartesian displacements $D^{Cart}_{\mathrm{ex}\,i}$ to the sum of intensities of fundamentals and to the total geometry changes, respectively. All values are normalized to unity (*ab intio* results: Δ,○; FC-fitted values: ▲,●).

FC fitting represent more than 80% of the square of total geometry changes, and the length of the relevant vector $\vec{D}^{\mathrm{Cart}}_{\mathrm{ex\,FCfit}}$ is larger than 0.9 of the total magnitude (length of the vector $\vec{D}^{\mathrm{Cart}}_{\mathrm{ex\,Tot}}$) of geometry change. Thus, the FC fitting presented in this article covers the major part of the total geometry change, even though only 7 from among 31 displacement parameters have been optimized. Moreover, the squares of Cartesian displacements of the three most important vibrations (253 cm^{-1}, 354 cm^{-1} and 418 cm^{-1}) contribute to 67% of the total sum of squares of the displacements, and the length of the relevant vector consisting of these three displacements exceeds 0.8 of the total magnitude of geometry change.

Franck–Condon fitting of band intensities increases the length of the H···O intramolecular hydrogen bond as well as the total magnitude of geometry changes computed by geometry optimization using the CC2 method by ca. 10% (see discussion in the Supplemental File). A similar analysis shows that the FC-fitted values are almost 50% larger than the pure DFT geometry changes.

The three in-plane modes discussed above represent essentially the rocking motions of the substituents or superposition of these motions with the simultaneous stretching or bending of the hydrogen bridge. The Potential Energy Distribution PED provides quantitative description of these modes in terms of the internal coordinates. The PEDs have been calculated using the GAR2PED program [54], with the set of non-redundant internal coordinates, as proposed by Pulay, Fogarasi and co-workers [55–57]. Typically, the valence bond lengths and the valence angles are used as internal coordinates. In this approach the PED for the investigated modes are as follows. The 253 cm^{-1} mode consists of: 55% of the rocking of the whole COOH group with respect to the benzene ring and roughly 20% of the rocking of the oxygen atoms with respect to the carbon atom within the carboxylic group. The 354 cm^{-1} mode consists of roughly 40% of the rocking of the whole NH_2 group with respect to the benzene ring and 20% of the benzene ring bending. The 418 cm^{-1} is essentially the combination of rocking of both substituents in the same direction, which leave the length of the hydrogen bond unchanged. This mode consists of roughly 33% of the rocking of the whole NH_2 group, 22% of the rocking of the oxygen atoms within the COOH group, and 20% of the benzene ring bending.

In an alternative approach to the PEDs of AA the hydrogen bond is treated in the same manner as the valence bonds, so the H-chelate ring is formed. In this picture both the 253 cm^{-1} and the 354 cm^{-1} modes consist of 80% of the O···H stretching. The

Table 4
Contributions of TDDFT modes to the CC2 modes for AA in the S_1 excited state for modes active in the LIF spectrum. Modes included in the FC fitting are bold.

CC2 modes freq./ cm^{-1}	contributions of TDDFT modes frequencies / cm^{-1}, contributions(%)
257	**260(100)**
362	**366(97)**
418	**418(99)**
492	504(98) **558(1)**
543	**558(99)** 504(1)
597	**615(100)**
710	**724(100)**
838	**851(100)**
1150	1164(96)
1201	1210(94)
1397	1379(42) 1450(28) 1342(14)

418 cm^{-1} mode is classified as the H-chelate ring bending mode (PED 75%), for which the comparison with the former approach to PEDs give a substantial value of the PED for the hydrogen bridge bending (N–H···O bending) equal roughly 20%. Thus, the modes included in the FC fitting comprises almost entire information concerning the changes of valence angles in the H-chelate ring as well as stretching and bending of the hydrogen bond, since the relevant contributions to potential energy dominate the PEDs of these modes and they are absent from the PEDs of other modes.

To achieve reliability of the FC-fitted geometry changes, the *ab initio* vibrational analysis should fulfill two important requirements. Firstly, the influence of Dushinsky effect on the modes included in the FC-fitting and having substantial contributions to the geometry changes should be small. This is certainly true for the in-plane modes of AA of frequencies below 900 cm^{-1} since the differences of the band intensities computed using the simple Δ-FC model ignoring the Dushinsky effect and with the MFC model, which takes this effect into account are small (a few% only). This is additionally confirmed by the analysis of the Dushinsky matrix. Squares of its diagonal elements are larger than 0.9 for the modes used in the FC fitting and they exceed 0.96 for the most important modes (253 cm^{-1}, 354 cm^{-1} and 418 cm^{-1}). Secondly, the *ab initio* vibrational analysis should provide quantitatively adequate description of molecular oscillations in terms of vibrational frequencies and mode pattern defined by displacements of atoms for each mode. Good agreement with the experimental data have been achieved for the vibrational frequencies of AA in the S_1 state computed with CC2 and TDDFT methods [34], including the most critical N–H stretching frequencies (detected experimentally by Southern et al. [14]). These methods proved its reliability during the analysis of isotopic shifts of vibrations active in the LIF spectrum of the isotopomers of AA [32] deuterated in the COOH and NH_2 groups. It indicated that for these modes the displacements of hydrogen atoms and the substituent groups are correctly predicted by the vibrational analysis based on these ab initio methods. This showed that the above methods (TDDFT and especially CC2) are able to provide the reliable prediction of vibrational modes that involve motions of the hydrogen bond and the substituent groups which are affected by large geometry changes.

The in-plane normal modes of frequencies below 900 cm^{-1} computed with the CC2 or TDDFT methods are virtually identical. The diagonal elements of the projection matrix of the normal coordinates computed with both methods (Table S3 in Supplemental file) are equal to 0.99–1.00 and the contributions of the relevant TDDFT modes to the CC2 modes are equal 97%−100% (Table 4). The above assures that the fitting of the relevant displacement parameters for the modes computed with both *ab initio* methods is carried out for essentially the same normal coordinates. The concurrence of the CC2 and TDDFT low-frequency in plane vibrations as well as the high-frequency OH and NH stretchings could be rationalized since the relevant modeling of the hydrogen bond between the substituents requires essentially the adequate modeling of dynamical correlation, which is achieved by both CC2 and DFT methods. Thus, both quantum chemistry methods provide adequate results of the modeling for the modes involving rocking of the COOH and NH_2 groups.

The opposite situation takes place for the middle-frequency modes (900–1800 cm^{-1}) which involves mainly skeletal stretchings of the π-electronic system (especially the aromatic ring) as well as the CH, OH and NH bendings. The adequate description of the electronic structure and dynamics of aromatic systems (especially in the excites states) requires the relevant treatment of the static correlations (near-degeneracy effects) and multiconfigurational nature of the electronic weavefunction. This is achieved by multiconfiguratioanl quantum chemistry methods, e.g. configuration interaction CI methods, coupled cluster as well as CASSCF/CASPT2 methods. For this issue, the CC2 approach performs significantly better than the TDDFT(B3LYP). Thus, it is not surprising that the discussed normal modes differs significantly between TDDFT and CC2 vibratioanl analysis (see Table S3 for the projection matrix in Supplemental file and Table S4 for contributions of normal modes).

6.3. Errors induced by the use of Cartesian coordinates

The transformations described in Section 4 (Eqs. (1)–(5)) are examined in order to estimate the errors of the FC-fitted geometry changes induced by the use of Cartesian coordinates. To summarize, in the approach described in Section 4 the transformations are carried out in three steps. Firstly, the displacement parameters for normal modes are computed according to Eqs. (3) and (4) on the basis of the following ab intio results: the computed geometry changes upon the electronic excitation and the normal modes resulting form vibrational analysis. In the second stage the displacement parameters are fitted are until band intensities in the experimental LIF spectrum are correctly reproduced. Finally, the FC-fitted geometry changes are calculated via the inverse transformation (Eq. (5)) from the optimized displacement parameters. Thus, the errors imposed by the use of Cartesian coordinates on the FC fitted geometry changes would cancel completely provided that the FC fitting does not change the initial values of the displacement parameters (and the geometry changes upon the electronic excitation) resulting from the ab initio computations. In this case, the cancellation of errors is exact, even though the description of normal modes in Cartesian coordinates could distort slightly the FC factors and the modeled intensities of vibronic bands. Because of the above, the errors of the FC-fitted geometry changes depend only on the magnitude of the refinement of the geometry changes which involve curvilinear motions, i.e. the changes of valence angles during the FC fitting. More specific analysis of these errors are presented below.

The calculation of displacement parameters is based on factorization of the geometry changes in terms of the displacements of atoms in normal modes. The errors are generated because the factorization of the bending distortions is carried out using the Cartesian approximation to the displacements of atoms in normal modes. Since the Cartesian displacements of atoms in numerical vibrational analysis are very small (order of magnitude 10^{-3} Å, which is relevant to the bending of valence angles by roughly 0.05°) they take place essentially along the tangent lines instead of the real curvilinear trajectories for bending modes. This results predominantly in the erroneous lengthening of bonds due to the distortion, which must be compensated by deviation from the original values for the displacement parameters Δ_i for the stretching modes involving these bonds. The above gives rise to erroneous

Table 5
Erroneous lengthening for bonds of length 140 pm induced by the use of Cartesian Coordinates for the description of variation of valence angles by $\Delta\alpha$, according to Eq. (10).

$\Delta\alpha$ /deg	ΔR_{err} /pm	$\Delta\alpha$ /deg	ΔR_{err} /pm
0.5	0.005	5.5	0.648
1.0	0.021	6.0	0.771
1.5	0.048	6.5	0.906
2.0	0.085	7.0	1.051
2.5	0.133	7.5	1.208
3.0	0.192	8.0	1.376
3.5	0.262	8.5	1.555
4.0	0.342	9.0	1.745
4.5	0.433	9.5	1.947
5.0	0.535	10.0	2.160

and inaccurate prediction of the FC factors and band intensities for stretching modes. Trigonometric considerations lead to the quantitative evaluation for the error of the bond lengths caused by the variation $\Delta\alpha$ of the angle α (formed by the group of atoms B–A–B'). The resulting erroneous bond length R' is given by Eq. (9).

$$R'(\Delta\alpha) = \frac{R}{\cos\Delta\alpha} \tag{9}$$

The maximum error in bond length ΔR_{err} given by Eq. (10) would be generated if the entire motion imposed by variation $\Delta\alpha$ concerns one atom (either B or B' atom).

$$\Delta R_{err}(\Delta\alpha) = R\left(\frac{1}{\cos\Delta\alpha} - 1\right) \tag{10}$$

The maximum errors calculated according to Eq. (10) for the bond of length 140 pm (the typical value for the C–C bonds in the aromatic system) are shown in Table 5. Errors approaching these values could induced by the C–H, N–H or O–H bendings that involve the motions of light hydrogen atom connected to the rather rigid molecular skeleton. Nevertheless, the errors are often smaller since the skeletal deformations usually (especially in the aromatic ring) causes displacements of both B and B' atoms. In the ideal case, if the magnitudes of displacements for both atoms are equal (½$\Delta\alpha$ for both atoms) the errors concerns both bond lengths (A–B and A–B') but they are four times smaller than the maximal ones due to approximately quadratic dependence of the errors on $\Delta\alpha$. Additional minor errors results from taking into account the length of linear displacements of atoms along the tangent lines in Cartesian coordinates instead of the length of the arc for curvilinear trajectories but these errors are negligible since they are smaller by 2–3 orders of magnitude than those resulting from Eq. (10).

For the AA molecule the refinements of valence angles during the FC fitting are small since they do not exceed 1° for the FC fitting aided by CC2 and 1.7° for the DFT-aided FC-fit (for comparison see results of the FC fitting presented in Sections 5.1 and 6.1 and the relevant ab initio results [34]). Assuming that the typical bond length in the aromatic ring is around 140 pm the maximum error ΔR is around 0.021 pm for the fitting aided by the CC2 results and 0.061 pm for the TDDFT fitting. Even though the above errors could propagate through the chain to remote bonds and their influences could accumulate, the resulting total errors remain small. Further geometric considerations were carried out to take into account the magnitude of changes of valence angles during the FC fitting and the fact that positions of atoms can be defined using at most two or three valence angles (starting from the C1 or C2 atom, which are located in the proximity of the center of inertia of the molecule). This leads to the conclusion that the total errors of bond lengths caused by the use of Cartesian coordinates instead of the curvilinear internal coordinates are smaller than 0.05 pm for the CC2-aided FC fitting and 0.15 pm for the TDDFT aided modeling. The above errors are very small and insignificant, especially in comparison with the discrepancies resulting from the use of different ab initio methods as well as the experimental errors.

Another important issue is whether the use of Cartesian coordinates could cause significant errors of the FC factors and the modeled intensities of the vibronic bands for the investigated transition in the AA molecule. On one hand, the changes of valence angles upon the electronic excitation in the AA molecule typically approach 5° (for skeletal angles in the aromatic system) and the largest change reaches 7.4° (C_2C_1N angle), therefore the errors of the FC factors and band intensities induced by the use of Cartesian coordinates may appear considerable. On the other hand, the real angular displacements of the skeleton atoms can be significantly smaller since the total change of relevant valence angle typically decomposes into motions of both part of the molecular skeleton connected thorough this valence angle.

The errors induced by the use of Cartesian coordinates could influence the intensities of the skeleton stretching modes and the C=O stretching, for which the FC modeling predicts small but discernible intensities (typically below 10% of I_{00}) and the ab initio calculations predict considerable genuine changes in the lengths of the relevant bonds (typically 3–5 pm), while the erroneous lengthening should be roughly 0.5 pm (see Table 5). On the other hand, the errors should influence the C–H, O–H and N–H_{free} stretchings as well, for which the ab initio calculations predict almost no changes in the bond lengths and the FC modeling predict negligible intensities (below 1% of I_{00}). The above suggests that these errors are not severe. These errors become significant for large changes of angles since the distortion by 15° generate erroneous lengthening of magnitude roughly 5pm. These errors could be significant in large molecules that consist of long and flexible (aliphatic) chains, in which positions and displacements of peripheral atoms depends on many valence and/or torsional angles, thus the errors cumulate. Probably, some part of intensities predicted by the ab initio methods for the many weak transitions involving the middle-frequency modes of the AA molecule (in the range 900–1800 cm^{-1}, see Table 1) could be induced by the errors related with the use of Cartesian coordinates. Fortunately, the predicted intensities of the relevant vibronic bands are small (typically smaller than 10% of I_{00}) and only three of these modes are observed in the experimental LIF spectrum (two of them are responsible for the presence of rather weak bands). Thus, the relevant displacement parameters have minor importance for the general intensity distribution in the modeled spectra. Moreover, their value cannot be neither confirmed (refined) quantitatively nor nullified on the basis of the experimental data. Nevertheless, these parameters should not be ignored and they were therefore kept frozen at values resulting directly from the ab initio calculations in order to retain many small contributions to the geometry changes, which in total cumulate to a considerable part of the investigated changes (see Section 6.4).

6.4. Geometry changes related to vibrations not included in the FC fitting

The displacement parameters Δ_i can be collected in two groups. The first one comprises the parameters for the seven in-plane modes of frequencies below 900 cm^{-1} that are fitted to the experimental band intensities and is related to the most prominent vibronic bands in the experimental spectrum. The second one comprises the parameters for the remaining in-plane modes which are not verified experimentally. The cumulated contributions of both these groups to the most important geometry parameters (according to the FC fit aided by the CC2/cc-pVTZ calculations) are shown in Table 6.

Table 6
Contributions of FC-fitted displacement parameters and remaining of geometry changes.

			total change	FC-fitted contributions		remaining contributions	
			/ pm, deg.	/ pm, deg.	% of total	/ pm, deg.	% of total
ΔR(A–B) / pm	aromatic ring	C_1–C_2	4.8	2.1	43	2.7	57
		C_3–C_4	4.5	1.3	29	3.2	71
		C_4–C_5	−0.8	0.3	−35	−1.1	135
		C_5–C_6	5.0	0.8	17	4.2	83
		C_1–C_6	−1.6	1.3	−83	−2.9	183
	substituents	C_1–N	0.2	0.5	240	−0.3	−140
		N–H_{free}	0.8	−0.4	−46	1.2	146
		N–H_{bond}	4.8	1.8	37	3.0	63
		C_2–C_7	−3.3	1.6	−49	−4.9	149
		C_7=*O*	3.7	1.6	43	2.1	57
		C_7–O	1.2	0.1	8	1.1	92
		O···H	−31.6	−24.1	76	−7.5	24
		O·····N	−14.0	−13.8	99	−0.2	1
angles / degrees	aromatic ring	C_2–C_1–C_6	4.5	2.9	65	1.6	35
		C_1–C_2–C_3	−3.1	−1.7	53	−1.4	47
		C_3–C_4–C_5	4.4	4.5	103	−0.1	−3
		C_4–C_5–C_6	−2.9	−2.6	89	−0.3	11
		C_1–C_6–C_5	−1.3	−1.1	87	−0.2	13
	substituents	C_2–C_1–N	−7.4	−5.8	79	−1.6	21
		C–N–H_{free}	0.9	1.0	112	−0.1	−12
		C–N–H_{bond}	−5.0	−1.4	28	−3.6	72
		C_3–C_2–C_7	3.2	2.6	81	0.6	19
		C_2–C_7=O	0.7	−0.3	−39	1.0	139
		N–H···O	15.0	9.1	61	5.9	39
		C=O···H	−3.4	−1.1	25	−2.5	75

The results shown in Table 6 are representative for all FC fits aided by the CC2 calculations since the discrepancies due to the use of various basis sets or FC models are small. The resulting contributions show that the seven most prominent displacement parameters optimized by the FC fitting contribute to the predominant part of the changes of skeletal angles and the shortening of the hydrogen bond. This results form the fact that the relevant oscillations represents mainly rocking and bending modes of substituents and skeletal bending modes of the aromatic ring (CCC bendings). Nevertheless, the contributions of the remaining modes are also substantial (often about 20%−40% of the total changes) and must not be ignored. The opposite situation takes place for the changes of lengths for valence bonds, the predominant part of which is included in the displacements for the remaining modes. Thus, it is not optimized on the basis of the experimental results via FC fitting and is solely based on the ab initio predictions.

The analogous distinction based on the FC fitting aided by the DFT calculations shows similar proportions of these contributions. The reliability of the FC-fitted results is proved by the consistency between the FC-fitted contributions to the geometry changes for the approaches aided by CC2 or DFT calculations. Unfortunately, the remaining parts of geometry changes based solely on the ab initio predictions differ from each other considerably. Nevertheless, the contributions based solely on the quantum chemistry results ought to be included in the complete modeling of geometry changes due to their significant magnitude, even though they give rise to the residual discrepancies between the final values of the estimated geometry changes.

Thus, the inverse modeling of geometry changes based on the FC fitting of band intensities in the vibronic spectra of AA (an example of polyatomic molecule) should be regarded as the approach that combines the quantum chemistry modeling and the experimental results. The approach presented in this work provides refinement of the predicted geometry changes, though they combine the two significant contributions: the experimentally verified geometry changes and the modeling of geometry changes using quantum chemistry computations.

7. Conclusions

Evaluations of the geometry changes upon the $S_0 \rightarrow S_1(\pi\pi^*)$ excitation in anthranilic acid (AA) have been carried out by fitting the reduced displacements along the normal coordinates until band intensities in the experimental LIF spectrum are correctly reproduced. The transformation of the reduced displacement parameters to the changes of equilibrium geometry has been facilitated by using of the theoretically obtained vibrational modes. They have been computed using two quantum chemistry methods: the CC2 coupled-cluster and TDDFT(B3LYP) with a series (aug)-cc-pVXZ(X = D,T,Q) basis sets. Such experimentally-based and theory-supported way of obtaining the geometry changes due to the electronic excitation have been subsequently examined for reliability, consistency and accuracy.

Consistency between the results obtained by the Franck–Condon fitting with the aid of CC2 or TDDFT(B3LYP) vibrational analysis proves that the experimentally-based (band intensities in the LIF spectrum) and theory-supported FC fitting procedure represents a reliable approach that provides quantitative estimation of the changes of equilibrium geometry upon the electronic excitation in the π-conjugated, internally H-bonded AA molecule. The theoretical calculations aided the analysis by providing consistent and correct description of oscillations involving rocking of the substituent groups and stretching or distortions of the intramolecular hydrogen bond. This has been achieved by the quantum chemistry methods that take into account the major part of the dynamic electron correlation and provide a qualitatively adequate description of the hydrogen bond in the excited electronic state.

The most reliable estimate for the shortening of the O···H bridge equals to 31 pm ± 1.5 pm (taking into account also the errors of the experimental band intensities) according to the LIF+CC2 MFC fitting. The values obtained using the above approach with various basis sets are scattered in the range 30.3–31.6 pm, while the relevant results estimated with the LIF+TDDFT FC fitting are roughly 1 pm smaller than the LIF+CC2 ones and are scattered in the range 29.3–30.6 pm. The residual discrepancy (roughly 1 pm) is small

in relative terms and it is comparable with other errors resulting from the use of different basis sets in vibrational analysis, or the use of the Δ-FC and the MFC models as well as the errors caused by inaccuracy of experimental band intensities. It seems that the predominant part of discrepancies between the geometry changes, as computed using the DFT and CC2 methods, is compensated by FC fitting to the experimental band intensities. These mutually corroborative estimations establish an important result concerning quantitative interpretation of the high resolution UV spectra for molecules of this kind, especially because in the earlier studies there were significant discrepancies between the estimates of the geometry changes [26,30,34]. The earlier estimates of the shortening of the O···H bridge varied from roughly 15 pm [30] (HF vs. CIS) through 19–23 pm [26,30,34] (DFT vs. TDDFT(B3LYP)) to over 30 pm [30] (LIF+DFT FC fit), thus the discrepancies exceeded 15 pm and 50% of the total magnitude of the investigated effect.

Generally, the geometry changes calculated with the LIF+TDDFT FC fitting are discernibly smaller than the LIF+CC2 ones. The most pronounced changes of valence angles (around 5–7°) are smaller by 0.5°−1.0° in the LIF+DFT approach, while the total variations of these changes due to the use of various basis sets in vibrational analysis do not exceed 0.3° (±0.15° from the average value). The values of the most prominent changes in bond alternation (of magnitude 5 pm) are typically 1 pm smaller when modeled with the LIF+TDDFT FC fitting than with the LIF+CC2 FC approach and they are scattered over 0.3 pm (±0.15 pm from the average value) at the most due to the use various basis sets in vibrational analysis.

The presented results indicate that the *ab initio* CC2 coupled-cluster computations provide remarkably good approximation of the geometry changes and very good staring point for the Franck–Condon fitting in the AA molecule, since the CC2-computed geometry changes [34] cover about 90% of the magnitude of the FC-fitted geometry changes. Thus, the geometry changes evaluated with the LIF+CC2 FC-fitting can be regarded as the more reliable and accurate than the LIF+TDDFT FC-fitting ones.

Nevertheless, the FC fitting aided by the TDDFT(B3LYP) vibrational analysis gives acceptable accuracy of estimation for the most pronounced geometry changes, despite the fact that the geometry changes obtained directly by means of DFT/TDDFT(B3LYP) geometry optimization for both electronic states were seriously underestimated [34]. It shows that sufficient accuracy of the fitting of geometry changes can be achieved using a relatively low-cost TDDFT methodology, without necessarily doing the more computationally demanding coupled clusters calculations.

Funding sources

This research was supported by:

- PL-Grid Infrastructure, with the calculations performed on Zeus: HP Cluster Platform of the Academic Computer Centre CYFRONET,
- The European Regional Development Fund and the Polish state budget within the framework of the Carpathian Regional Operational Programme (RPPK.01.03.00-18-001/10) through the funding of the Centre for Innovation and Transfer of Natural Science and Engineering Knowledge of the University of Rzeszów.

Supporting information

The Supporting Information file contains Tables S1 and S2 presenting Franck–Condon modeling of intensities for the fundamental bands computed on the basis of CC2 and TDDFT quantum chemistry calculations, respectively, with the series of (aug)-cc-pVXZ(X = D,T,Q) basis sets and within both the ΔFC and MFC models of Franck–Condon factors. Table S3 presents projection matrix of the virational modes computed with CC2 and TDDFT methods and Table S4 shows the contributions of the CC2 and TDDFT modes. Additionally, more extensive discussion of the geometry changes is included.

Declaration of Competing Interest

None.

Supplementary materials

Supplementary material associated with this article can be found, in the online version, at doi:10.1016/j.jqsrt.2019.106747.

CRediT authorship contribution statement

Przemysław Kolek: Conceptualization, Data curation, Formal analysis, Investigation, Writing - original draft, Writing - review & editing. **Marcin Andrzejak:** Data curation, Formal analysis, Investigation, Writing - original draft, Writing - review & editing. **Tomasz Uchacz:** Conceptualization, Investigation, Writing - original draft, Writing - review & editing. **Paweł Szlachcic:** Conceptualization, Investigation, Writing - original draft, Writing - review & editing.

References

[1] Dierksen M, Grimme S. Density functional calculations of the vibronic structure of electronic absorption spectra. J Chem Phys 2004;120:3544–54.
[2] Barone V, Bloino J, Biczysko M, Santoro F. Fully integrated approach to compute vibrationally resolved optical spectra: from small molecules to macrosystems. J Chem Theory Comput 2009;5:540–54.
[3] Santoro F, Lami A, Improta R, Barone V. Effective method to compute vibrationally resolved optical spectra of large molecules at finite temperature in the gas phase and in solution. J Chem Phys 2007;126(1–11):184102.
[4] Bloino J, Biczysko M, Crescenzi O, Barone V. Integrated computational approach to vibrationally resolved electronic spectra: anisole as a test case. J Chem Phys 2008;128(1–15):244105.
[5] Santoro F, Lami A, Improta R, Bloino J, Barone V. Effective method for the computation of optical spectra of large molecules at finite temperature including the duschinsky and herzberg–teller effect: The q_x band of porphyrin as a case study. J Chem Phys 2008;128(1–17):224311.
[6] Baiardi A, Bloino J, Barone V. General time dependent approach to vibronic spectroscopy including franck-condon, herzberg-teller, and duschinsky effects. J Chem Theory Comput 2013;9:4097–115.
[7] Santoro F, Mortaheb F, Lepelmeier J, Boesl U, Heiz U, Kartouzian A. High-resolution absorption and electronic circular dichroism spectra of (R-+)-1-phenylethanol. confident interpretation based on the synergy between experiments and computations. ChemPhysChem 2018;19:715–23.
[8] Stuhlmann B, Grassle A, Schmitt M. Determination of the geometry change of 5-cyanoindole upon electronic excitation from a combined franck-condon/rotational constants fit. Phys Chem Chem Phys 2014;16:899–905.
[9] Gmerek F, Stuhlmann B, Alvarez-Valtierra L, Pratt DW, Schmitt M. Electronic spectra of 2- and 3-tolunitrile in the gas phase. II. geometry changes from franck-condon fits of fluorescence emission spectra. J Chem Phys 2016;144(1–8):084304.
[10] Hebestreit M-L, Henrichs C, Schneider M, Wilke M, Meerts WL, Krügler D, Schmitt M. Structural changes upon electronic excitation in 1,2-dimethoxybenzene from rotationally resolved electronic spectroscopy of various isotopologues. J Mol Struct 2019;1184:139–45.
[11] Turchiello RF, Lamy-Freund MT, Hirata IY, Juliano L, Ito AS. Ortho-aminobenzoic acid as a fluorescent probe for the interaction between peptides and micelles. Biophys Chem 1998;73:217–25.
[12] Ito AS, Turchilleo RF, Hirata IY, Cezari MHS, Meldal M, Juliano L. Fluorescent properties of amino acids labeled with ortho-aminobenzoic acid. Biospectrosopy 1998;4:395–402.
[13] Stalin T, Rajendiran N. Intramolecular charge transfer associated with hydrogen bonding effects on 2-aminobenzoic acid. J Photochem Photobiol A 2006;182:137–50.
[14] Southern CA, Levy DH, Florio GM, Longarte A, Zwier TS. Electronic and infrared spectroscopy of anthranilic acid in a supersonic jet. J Phys Chem A 2003;107:4032–40.
[15] Stearns JA, Das A, Zwier TS. Hydrogen atom dislocation in the excited state of anthranilic acid: probing the carbonyl stretch fundamental and the effects of water complexation. Phys Chem Chem Phys 2004;6:2605–10.
[16] Weller A. Fast reactions of excited molecules. Prog React Kinet Mech 1961;1:187–97.
[17] Heimbrook L, Kenny JE, Kohler BE, Scott GW. Lowest excited singlet-state of hydrogen bonded methyl salicylate. J Phys Chem 1983;87:280–9.

[18] Bisht PB, Petek H, Yoshihara K, Nagashima U. Excited state enol-keto tautomerization in salicylic acid: a supersonic free jet study. J Chem Phys 1995;103:5290–307.
[19] Nagaoka S, Nagashima U. Intramolecular proton transfer in various electronic states of otho-hydroxybenzaldehyde. Chem Phys 1989;136:153–63.
[20] Lahmani F, Zehnacker-Rentien A. Effect of substitution on the photoinduced intramolecular proton transfer in salicylic acid. J Phys Chem A 1997;101:6141–7.
[21] Peteanu LA, Mathies RA. Resonance raman intensity analysis of the excited-state proton transfer in 2-hydroxyacetophenone. J Phys Chem 1992;96:6910–16.
[22] Herek JL, Pedersen S, Banares L, Zewail AH. Femtosecond real-time probing of reactions. IX. hydrogen-atom transfer. J Chem Phys 1992;97:9046–61.
[23] Vener MV, Scheiner S. Hydrogen bonding and proton transfer in the ground and lowest excited singlet states of o-hydroxyacetophenone. J Phys Chem 1995;99:642–9.
[24] Sobolewski AL, Domcke W. Ab initio potential-energy functions for excited state intramolecular proton transfer: a comparative study of o-hydroxybenzaldehyde, salicylic acid and 7-hydroxy-1-indanone. Phys Chem Chem Phys 1999;1:3065–72.
[25] Sobolewski AL, Domcke W. Ab initio study of excited-state intramolecular proton dislocation in salicylic acid. Chem Phys 1998;232:257–65.
[26] Sobolewski AL, Domcke W. Intramolecular hydrogen bonding in the S1($\pi\pi^*$) excited state of anthranilic acid and salicylic acid: tddft calculation of excited-state geometries and infrared spectra. J Phys Chem A 2004;108:10917–22.
[27] Sobolewski AL, Domcke W. On the mechanism of rapid non-radiative decay in intramolecularly hydrogen-bonded pi systems. Chem Phys Lett 1999;300:533–9.
[28] Kolek P, Lesniewski S, Pirowska K, Najbar J. LIF excitation spectra for S0→S1 transition of anthranilic acid: Detailed studies. J Mol Spectr 2008;249:100–12.
[29] Wu C, He Y, Kong W. Two-color two-photon rempi and zeke spectroscopy of supersonically cooled o-aminobenzoic acid. Chem Phys Lett 2004;398:351–6.
[30] Lesniewski S, Kolek P, Pirowska K, Sobolewski AL, Najbar J. Franck-Condon analysis of laser-induced fluorescence excitation spectrum of anthranilic acid: Evaluatioan of geometry change upon S0→S1 excitation. J Chem Phys 2009;130(1−14):054307.
[31] Kolek P, Lesniewski S, Andrzejak M, Gora M, Cias P, Wegrzynowicz A, Najbar J. LIF excitation spectra for S0→S1 transition of deuterated anthranilic acid (COOD, ND2) in supersonic-jet expansion. J Mol Spectr 2010;264:129–36.
[32] Kolek P, Andrzejak M, Najbar J, Ostrowska-Kopeć M, Piotrowska I. Isotopic effects in the S1 exited state of anthranilic acid deuterated in various positions in substituent groups. supersonic-jet lif spectroscopy and CC2 ab initio study. Chem Phys 2015;450:46–58.
[33] Andrzejak M, Kolek P. Theoretical modeling of deuteration-induced shifts of the 0−0 bands in absorption spectra of selected aromatic amines: The role of the double-well potential. J Phys Chem A 2013;117:12770–82.
[34] Kolek P, Andrzejak M, Hakalla R, Szajna W. Quantitatively adequate calculations of the H-chelate ring distortion upon the S0 → S1($\pi\pi^*$) excitation in internally H-bonded o-anthranilic acid: CC2 coupled-cluster versus tddft. J Phys Chem A 2018;122:6243–55.
[35] Araki M, Motylewski T, Kolek P, Maier JP. Electronic absorption spectrum of a nonlinear carbon chain: trans-$C_6H_4^+$. Phys Chem Chem Phys 2005;7:2138–41.
[36] Khoroshev BD, Araki M, Kolek P, Birza P, Chirokolava A, Maier JP. Rotationally resolved electronic spectroscopy of a nonlinear carbon chain radical $C_6H_4^+$. J Mol Spectr 2004;227:81–9.
[37] Araki M, Linnartz H, Kolek P, Ding H, Boguslavskiy A, Denisov A, Schmidt TW, Motylewski T, Cias P, Maier JP. New laboratory data on a molecular band 4429 a. Astrophys. J 2004;616:1301–10.
[38] Frisch MJ, Trucks GW, Schlegel HB, Scuseria GE, Robb MA, Cheeseman JR, Scalmani G, Barone V, Mennucci B, Petersson GA, et al. *Gaussian 09*, Revision E.1. Wallingford, CT: Gaussian, Inc.; 2009.
[39] Christiansen O, Koch H, Jørgensen P. The second-order approximate coupled cluster singles and doubles model CC2. Chem Phys Lett 1995;243:409–18.
[40] Hättig C. Geometry optimizations with the coupled-cluster model CC2 using the resolution-of-the-identity approximation. J Chem Phys 2003;118:7751–61.
[41] Köhn A, Hättig C. Analytic gradients for excited states in the coupled-cluster model CC2 employing the resolution-of-the-identity approximation. J Chem Phys 2003;119:5021–36.
[42] Andrzejak M, Orzeł Ł. Joint theoretical and experimental study on the phosphorescence of 2,2 '-bithiophene. Phys Chem Chem Phys 2014;16:5605–6512.
[43] Andrzejak M, Szczepanik D, Orzeł Ł. The lowest triplet states of bridged cis-2,2 '-bithiophenes - theory vs. experiment. Phys Chem Chem Phys 2015;17:5328–37.
[44] TURBOMOLE V6.3 2011, a development of University of Karlsruhe and Forschungszentrum Karlsruhe GmbH, 1989−2007, TURBOMOLE GmbH, since 2007; http://www.turbomole.com.
[45] Coon JB, DeWames RE, Loyd CM. Franck-Condon principle and structures of excited electronic states of molecules. J Mol Spectr 1962;8:285–305.
[46] Henderson JR, Muramoto M, Willett RA. Harmonic franck-condon overlap integrals including displacements of normal coordinates. J Chem Phys 1964;41:580–99.
[47] Sharp TE, Rosenstock HM. Franck-Condon factors for polyatomic molecules. J Chem Phys 1964;41:3453–73.
[48] Doktorov EV, Malkin IA, Man'ko VI. Dynamical symmetry of vibronic transitions in polyatomic molecules and franck-condon principle. J Mol Spectr 1975;56:1–20.
[49] Gruner D, Brumer P. Efficient evaluation of harmonic polyatomic franck-condon factors. Chem Phys Lett 1987;138:310–14.
[50] Ruhoff PT. Recursion relations for multidimensional franck-condon overlap integrals. J Chem Phys 1994;186:355–74.
[51] Ruhoff PT, Ratner MA. Algorithms for computing franck-condon overlap integrals. Int J Quant Chem 2000;77:383–92.
[52] SCILAB 4.0, 2006, INRIA ENPC, www.scilab.org.
[53] Reimers JR. A practical method for the use of curvilinear coordinates in calculations of normal-mode-projected displacements and duschinsky rotation matrices for large molecules. J Chem Phys 2001;115:9103–9.
[54] Martin, J.M.L.; Van Alsenoy, C. Gar2ped, a program to obtain a potential energy distribution from a Gaussian archive record 2007.
[55] Pulay P, Fogarasi G, Pang F, Boggs JE. Systematic ab initio gradient calculation of molecular geometries, force constants, and dipole moment derivatives. J Am Chem Soc 1979;101:2550–60.
[56] Fogarasi G, Zhou X, Taylor PW, Pulay P. The calculation of ab initio molecular geometries: efficient optimization by natural internal coordinates and empirical correction by offset forces. J Am Chem Soc 1992;114:8191–201.
[57] Pulay P, Fogarasi G. Geometry optimization in redundant internal coordinates. J Chem Phys 1992;96:2856–60.